Geochemical insights into spatial and temporal evolution of sediment at catchment scale (Egoutier stream, France)

Lauriane Ledieu, Anaëlle Simonneau, Olivier Cerdan, Philippe Négrel, Valérie Laperche, Cécile Grosbois, Fatima Laggoun-Défarge

Journal Pre-proof

GEOCHEMICAL INSIGHTS INTO SPATIAL AND TEMPORAL EVOLUTION OF SEDIMENT AT CATCHMENT SCALE (Egoutier stream, France)

L. Ledieu, A. Simonneau, O. Cerdan, P. Négrel, V. Laperche, C. Grosbois, F. Laggoun-Défarge

PII: S0883-2927(20)30235-3

DOI: https://doi.org/10.1016/j.apgeochem.2020.104743

Reference: AG 104743

To appear in: *Applied Geochemistry*

Received Date: 20 December 2019

Revised Date: 21 August 2020

Accepted Date: 21 August 2020

Please cite this article as: Ledieu, L., Simonneau, A., Cerdan, O., Négrel, P., Laperche, V., Grosbois, C., Laggoun-Défarge, F., GEOCHEMICAL INSIGHTS INTO SPATIAL AND TEMPORAL EVOLUTION OF SEDIMENT AT CATCHMENT SCALE (Egoutier stream, France), *Applied Geochemistry*, https://doi.org/10.1016/j.apgeochem.2020.104743.

GEOCHEMICAL INSIGHTS INTO SPATIAL AND TEMPORAL EVOLUTION OF SEDIMENT AT CATCHMENT SCALE (Egoutier stream, France)

L. Ledieu[1], A. Simonneau[1], O. Cerdan[2], P. Négrel[2], V. Laperche[2], C. Grosbois[3], F. Laggoun-Défarge[1]

[1]Univ. Orléans, CNRS, BRGM, ISTO, UMR 7327, F-45071, Orléans, France
[2]BRGM, 3 avenue Claude Guillemin, 45060 Orléans, France
[3]GéHCO, University of Tours, 37200 Tours, France

Abstract

The transfer and storage of chemical elements in particulate matter are controlled by physical, chemical and biological processes. Their dynamics are well understood, especially in environments that show strong tectonic and/or geomorphic pressures, and are frequently reconstructed over centuries or decades to evaluate climate change effects for example. However, observations carried out at high spatial and temporal resolutions are less common, particularly in lowland areas. The present study aimed to better understand the links between earth surface processes, such as soil weathering and erosion, by combining pedology, geochemistry and hydrology at a small catchment scale. It focuses on the transfer of selected chemical elements (Ca, K, Ti, Fe, Mn, Rb and Sr) associated with particulate erosion and transport. The first (topsoil) and last (subsoil) soil horizons from different soil profiles and stream bed-load sediments of the Egoutier catchment (8 km², Loiret, France) were studied. The objective was to investigate the relationship between the weathering and erosion processes. The soils are developed on ancient alluvium as evidenced by their physical and chemical properties, which clearly displayed a weathering profile from bedrock to topsoil layers. Ca, Fe and Rb showed migration dynamics from the topsoils to the subsoils, whereas Mn appeared immobilized within topsoils. Enrichments of all investigated elements increased in bed-load sediments. Topsoil erosion is the main source of sediment. However, Fe and Rb enrichments also highlight the remobilization of subsoils during periods of enhanced precipitation. Furthermore, Fe and Rb enrichments show a selective erosion of clay minerals. K and Sr contents evidence mineral break-up processes favoring mechanical erosion of all mineral phases. Moreover, their enrichments can be interpreted as the result of higher erosion rates and deposition during high rainfall events. The same conclusion can be drawn for Mn and Ca although their spatial variabilities depend on contributions from runoff in urban areas, as

rainwaters from anthropized areas supply Ca mineral phases and diluted Mn depleted bearing phases from topsoil layers.

Keywords

Weathering, Erosion, Soil, Sediment, Geochemistry

1. Introduction

The Critical Zone (CZ) is defined as the thin layer of the Earth's surface and near-surface terrestrial environment. This zone forms the link between rocks, soils, atmospheric gases and meteoric waters, which are the habitat of humanity and biodiversity (Anderson et al., 2007). The storage and transfer of waters and chemical elements in these compartments are controlled by complex physical, chemical and biological processes (Négrel et al., 2018a) leading to vertical and lateral heterogeneities of the CZ. To better understand the behavior of this sensitive compartment, we need to combine disciplines such as geochemistry, pedology and hydrology (Richter et al., 2015) and to evaluate the spatial and temporal evolutions of its physical and chemical properties (Pierret et al., 2018).

At catchment scale, some CZ compartments, such as soils, act as a sink with large capacities of storage for many chemical elements (Kabata-Pendias and Pendias, 2001), while other compartments, such as river bed-load sediments, are crucial vectors for element transport (Oelkers et al., 2011). As underlined by Nesbitt et al. (1980), in order to achieve full knowledge of sedimentary cycle geochemistry, documentation about the behavior of chemical elements during weathering is required. In the 19th century, soils were defined as dynamic sensitive systems responding to natural environmental forcings, whose weathering mainly depends on climate forcing (Pickering, 1986; Richter et al., 2015) and rainfall amounts (Defersha and Melesse, 2012), especially in tropical (Silva et al., 2018; Yang and Zhang, 2019) and glacial (Bernasconi et al., 2008; Heindel et al., 2018; Marerro et al., 2018) environments. Considering that soil elemental composition is also driven by the bedrock composition (Pickering, 1986), detailed descriptions of weathering processes were done on specific bedrocks and/or mineral phases (Harriss and Adams, 1966; Johnson et al., 1968; Cleaves et al., 1970).

As strong links exist between chemical weathering and physical erosion (Emberson et al., 2016), integrated studies evaluating the geochemistry of bed-load sediments related to their direct bedrock or soil sources thus started to be developed (Martin and Meybeck, 1979; Cullers et al., 1987; Cullers, 1988). Nevertheless, most of the studies were carried out at a global scale and encountered difficulties making the link between weathering and erosion processes because of the complexity induced by the potential interaction of different phenomena : absorption, retention, fractionation, transport, and deposition (Bormann and Likens, 1967; Nesbitt et al., 1980; Cullers, 1988). As these processes can operate independently, together or sequentially (Butt, 1992), their respective effects are difficult to distinguish. This is even more the case in environments with variable lithologies and a relationship between surface and groundwaters (Bormann and Likens, 1967) where the contributions of the different bedrocks and elemental cycles through groundwaters are hard to establish.

To assist in the characterization of soil and water geochemical cycles, the concept of individual catchment units was defined (Likens and Cowan Jr, 1992). In a watershed ecosystem, geochemical inputs have meterological and biological origins, while outputs have biological and geological ones. The differences between the inputs and outputs therefore provide insight into weathering and erosion dynamics (Bormann and Likens, 1967). Catchment outputs are linked to dissolved and particulate material originating from chemical and physical erosion (Nelson, 1973). At catchment scale, multi-elemental chemistry analysis of water, soils and bed-load sediments, compared to the bedrock signature (Cullers et al., 1988; Négrel and Deschamps, 1996; Grosbois et al., 2000) become widely used. Given the crustal abundance of silicate rocks (Parker, 1967) and their weathering recycling role for atmospheric CO2 (Brady, 1991), riverine particulate transport associated to weathered silicate bedrocks has recently received attention (Viers et al., 2009). Directly linked to their geochemistry, sediment rates, textural and mineralogical characteristics are driven by soil erosion. Because erosion rates are enhanced under strong topographic and anthropogenic forcings (Delmas et al., 2012), many studies have focused on mountainous (Gaillardet et al., 1999; Emberson et al., 2016) or agricultural areas (Marshall and Bayliss, 1994; Grosbois et al., 2000; Cerdan et al., 2002). As a result of increasing urbanization, urban geology has started to emerge as a discipline (Wilson and

Jackson Jr., 2016). Growing funds and legislative demands to improve knowledge of urban areas has enabled the development of geochemical mapping in this kind of environment (Johnson and Ander, 2008). Nevertheless, only a few studies on erosion have been carried out in peri-urban areas (Rowntree et al., 1991; Grau et al., 2008). Although subjected to rapid transformations, these anthropogenic zones are nevertheless important actors in modifications of biogeochemical cycles (Douglas, 2012).

To evaluate the horizontal and lateral evolutions and transportability of chemical elements in the sedimentary cycle, from bedrock to sediments, more information is needed. It is necessary to distinguish whether existing observations are ubiquitous or site-dependent, suggesting specific controlling factors. The determination of the predominant controlling factors is possible by observing of weathering and erosion processes in small peri-urban catchments. Small watershed studies are manageable (Nelson, 1973), present fewer variabilities (Likens and Cowans Jr, 1992) and avoid scale effect smoothing, thus enabling high spatial and temporal characterization of the processes driving biogeochemical cycles.

The present study was conducted at a small catchment scale (Egoutier, 8 km²) with homogeneous bedrock to decipher weathering dynamics and the continuum of erosion processes and to improve the understanding of particle evolution by the textural, mineralogical and geochemical characterization of soil and sediments. Conducted on varying landscapes on hydromorphic sandy-clay soils and on bed-load sediments derived from different rainfall events in a small stream, this research defines forcing effects in a peri-urban lowland area. It allowed the source contributions to be reconstructed and/or specific processes to be traced at a low temporal scale.

2. Materials and methods

2.1 Study site and sampling

The Egoutier stream is located in the Loire River basin near Orleans (Loiret, France, Fig. 1). The Egoutier is a tributary of the Loire River draining a small catchment (27 km²) collecting pluvial and sewage networks. In this study, we restricted the investigation area to the upstream part of the catchment covering 8 km². It has a temperate climate, with an average annual rainfall in the area of

650 mm (Soucémarianadin and Verbèque, 2007). Depending on stormwaters and soil saturated runoff, the location of the Egoutier source can vary according to the season and/or the rainfall regime. The upstream eastern stream (dotted line, Fig. 1) is for instance only effective during periods of enhanced precipitation. In the northern part, the stream is also fed by two sewage water effluents: one from a Central Army Pharmacy (CAP, Fig. 1), and another from a psychiatric hospital (PH, Fig. 1).

[Figure 1]

Figure 1: Characteristics of the study site and location of the samples: types of soils and location of the soil surveys (A), land covers, location of the artificial supplies to the watercourse and of the bed-load sediment samples (B)

The mean slope gradient of the catchment is 0.5 %. The upstream to downstream substratum is composed of Sologne sands and clays (SSC), Orleanais sands (OS), Burdigalian fluvial deposits dated 21.5 to 16.3 Ma and Beauce limestone dated 23.3 to 21.5 Ma (Berger and Desprez, 1969, Fig. 1). The streambed is impermeable because of clay-rich subsoil horizons (Soucémarianadin and Verbèque, 2007; Fig. 1). Land cover is mainly forests (74 % of the total surface, Fig. 1) and anthropized areas with residential (12 %, Fig. 1), agricultural (7 %, Fig. 1) and industrial zones (4 %, Fig. 1). One pond (the Beulie pond) is present in the central part of the catchment area.

Soil surveys (yellow stars, Fig. 1) were conducted for each type of soil and under each land cover type. Following Soucémarianadin and Verbèque (2007), Redoxisol, Planosol and Brunisol (French classification; Baize et al., 2009) cover 95 %, 4% and 1 % of the area, respectively. 13 soil profiles were collected in April 2018 with a hand soil auger and the maximum depth was limited to the homogeneous impermeable subsoil layer. Each horizon was described and sampled but only the top and bottom layers of each profile were analyzed (topsoil and subsoil, respectively). Bed-load sediments (BLS) were collected from upstream to downstream all along the watercourse (orange circles, Fig. 1), paying attention to each confluence. A total of 8 samples were collected in February and March 2017 and replicated in April 2018 (Fig. 1).

2.2 Quantification of chemical elements

Elemental concentration measurements of all collected samples (soils and BLS) were performed by X-Ray Fluorescence spectrometry (XRF) with a NITON XL3t980 GOLDD fitted with a 50 kV X-ray tube (max. 50 kV, 100 µA, 2 W) with an Ag anode target excitation source and a Large Drift Detector (LDD). As part of the standard set-up routine and to avoid contamination, the analyzer was initially Energy calibrated using the embedded Silver target. Samples were dried at 50 °C during 48 hours, crushed in an agate mortar and sieved under 200 µm to have a homogeneous overview of the bulk geochemistry. XRF sample cups with 10-15g of powder were analyzed through 6 µm Mylar films and with an average analyzed spot diameter of 8 mm. The mining mode calibration done by the manufacturer was used for all analyses and source count time was fixed at 90 seconds using the 3 filters of the pXRF in the laboratory (30 seconds for each filter). Three certified standards (NIST2710a, NIST2711a, NIST2780) were used to verify the calibration and calculate correction factors (Table 1). Each sample was analyzed three times to determine the reproducibility of the measurements (Table 1). In order to highlight different processes, only seven elements were selected in this study in relation with their particular behavior: soluble elements such as calcium (Ca), potassium (K), strontium (Sr) and rubidium (Rb); an insoluble one: titanium (Ti); and two redox sensitive ones: iron (Fe) and manganese (Mn). These elements enable mineral contributions to be tracked as they are often associated to silicates (K, Rb, Ti), carbonates (Ca, Sr, Negrel and Grosbois, 1999), clays (K, Fe, Mn, Pickering, 1986), and metal oxi-hydroxides (Fe, Mn, Kabata-Pendias and Pendias, 2001).

Table 1: Certified standards mean contents (mg/g) and % standard deviations (National Institute of Standards and Technology), derived correction factors and % samples mean deviations

Element	Certified standards mean contents (NIST2710a/ NIST2711a/ NIST2780)	Certified standard deviations (NIST2710a/ NIST2711a/ NIST2780)	Correction factors	Samples mean deviations
K	21.7 / 25.3 / 33.8	6.0 / 3.9 / 7.7	1.0 / 1.0 / 1.0	0.6
Ca	9.6 / 24.2 / 1.9	4.7 / 2.5 / 10.3	0.8 / 1.0 / 0.7	0.5
Ti	3.1 / 3.2 / x	2.2 / 2.5 / x	0.8 / 1.1 / x	1.2
Fe	43.2 / 28.2 / 27.8	1.8 / 1.4 / 2.9	1.0 / 1.1 / 0.9	0.6
Mn	2.1 / 0.7 / 0.5	2.8 / 2.7 / 4.5	0.2 / 1.2 / 0.9	4.9
Rb	0.12 / 0.12 / x	2.6 / 0.5 / x	0.9 / 1.1 / x	1.4
Sr	0.26 / 0.24 / 0.22	2.7 / 4.1 / 8.3	0.8 / 1.1 / 0.9	1.7

Multivariate statistical analysis can provide precious informations about the correlations between different variables (Zhang and Selinus, 1998; Reimann et al., 2002). A Principal Component Analysis (PCA) was therefore conducted using XLSTAT with topsoil and subsoil layers geochemical results to visualize any correlations between each chemical element and its distribution in the soil sample set. Moreover, soil typologies, land cover and bedrock were represented as additional variables to see their potential effect on the distribution of chemical elements. The PCA had a p-value < 0.0001 at the Bartlett sphericity test, and a Kaiser-Meyer-Olkin sample adequacy of 0.437. Data set statistical parameters are resumed in Table 2.

170 *Table 2: Variables contribution (%) to the first (F1) and the second (F2) principal components of the PCA before and after the*
171 *varimax rotation, and the p-value of the Shapiro-Wilk test*

	K	Ca	Ti	Fe	Mn	Rb	Sr
Variables contribution to F1	26.9	0.1	5.9	28.7	17.2	8.6	12.6
Variables contribution to F2	5.0	31.6	14.8	5.5	1.6	27.1	14.4
Variables contribution to F1 after varimax rotation	30.9	8.4	17.2	10.0	7.7	0.2	25.6
Variables contribution to F2 after varimax rotation	3.8	18.0	1.2	29.1	14.2	33.6	0.1
p-value of the Shapiro-Wilk test	0.289	0.031	0.032	0.120	0.002	0.590	0.050

172

173 Enrichment factors (EF) are traditionally used to evaluate chemical changes due to alteration-
174 erosion processes (Ghadiri and Rose, 1991; Négrel and Deschamps, 1996; Négrel, 1999) and
175 contamination levels (Barbieri, 2016), or to highlight losses (nutrients, Palis et al., 1990). For soils-
176 sediments, EF are calculated by dividing the element content in the eroded sediment by its content in
177 the original soil (Barrows and Kilmer, 1963). Basic EF can be improved by a normalization with a
178 conservative element such as Al, Li, Sc, Zr, or Ti. This conservative element must show weak
179 variability within the sample set and should not be affected by weathering processes (Reimann and
180 Caritat, 2005). Moreover, it must be free from particle size effects and/or fractionation by any
181 processes. Ti is often a good candidate to carry out this normalization (Zr being another one). Here EF
182 were calculated as follows:

183 $$EF = \frac{\left(\frac{[El]}{[Ti]}\right)_{sample}}{\left(\frac{[El]}{[Ti]}\right)_{reference}} \qquad \text{Eq. 1}$$

184 *2.3 Mineralogical and textural analysis*

185 Bulk mineralogy was determined by X-Ray Diffraction spectrometry (XRD) at ISTO laboratory on ten
186 samples (two topsoils, two subsoils and three BLS samples from each of the two surveys dating from
187 2017 and 2018, respectively, Fig. 1). The BLS sampled in 2017 were analyzed using a Thermo-
188 Electron Bruker D8 Advance diffractometer, whereas the others were characterized using an INEL
189 diffractometer with a Debye-Scherrer configuration. The diagrams obtained were compared to the
190 characteristic diagrams of the ICDD (International Centre for Diffraction Data) PDF (Powder
191 Diffraction File). It allowed to identify the presence of mineral phases but this method was only
192 qualitative.

193 Textures were determined by granulometric analysis. For all samples, the moistened fraction
194 under 1.6 mm was analyzed by a laser particle sizer Mastersizer 3000. The relative percentages of four
195 grain-size classes were quantified: 0-2 µm as clay size fraction, 2-63 µm as silt size fraction, 63-
196 200/250 µm as fine sand size fraction and 200/250-1600 µm as medium to coarse sand size fraction.

197 **3. Results**

198 *3.1 Soils and sediments geochemistry*

199 K and Fe were the most abundant elements in topsoils, with concentrations ranging from 15.7 to 23.8
200 mg/g and from 4.6 to 24.6 mg/g, respectively (median content of 19.0 and 13.8 mg/g, respectively;
201 Fig. 2). Ca content did not exceed 9.4 mg/g (median content of 4.4 mg/g; Fig. 2) and was the lowest
202 major element. Ti ranged from 5.2 mg/g to 8.6 mg/g (median content of 6.4 mg/g; Fig. 2). Considered
203 as trace element because of its concentrations, Mn was the most abundant but also the most dispersed,
204 with concentrations ranging from 0 to 1.24 mg/g (median content of 0.39 mg/g; Fig. 2). Sr was the

least abundant, with values between 0.05 and 0.07 mg/g (median content of 0.06 mg/g; Fig. 2) and Rb ranged from 0.10 to 0.16 mg/g (median content of 0.13 mg/g; Fig. 2).

Similar variations in a higher range of concentrations were observed in the subsoils. Fe and K were still the two most abundant elements, with concentrations ranging from 17.8 to 42.8 mg/g and from 14.7 to 21.4 mg/g, respectively (median content of 29.0 and 17.1 mg/g, respectively; Fig. 2). Ca was still the least abundant varying from 2.5 to 10.8 mg/g (median content of 5.1 mg/g; Fig. 2), while Ti concentrations ranged from 5.7 to 7.3 mg/g (median content of 6.1 mg/g; Fig. 2). Trace elements also presented similar variations to the topsoil samples. Mn was still the most dispersed element ranging from 0 to 0.57 mg/g (median content of 0.19 mg/g; Fig. 2) but had the highest concentrated in only two soil surveys (S9 and S12, Fig. 1). In other soil profiles, Rb presented higher concentrations, between 0.15 and 0.21 mg/g (median content of 0.18 mg/g; Fig. 2). Sr was still the least abundant element with ontents varying from 0.05 to 0.07 mg/g (median content of 0.06 mg/g; Fig. 2).

[Figure 2]

Figure 2: Median values (and standard deviation values) of iron, calcium, potassium, titanium, strontium, rubidium and manganese in topsoils (a) and subsoils (b) of each soil described in the catchment area and bed-load sediment samples (BLS, c). The typology of each soil is mentioned in figure 1.

The BLS samples showed different trends (Fig. 2). In 2017, Ca was the major element, with concentrations ranging from 2.7 to 130.0 mg/g (median content of 28.6 mg/g; Fig. 2) but also the most dispersed. Ti concentrations were the lowest, varying from 1.1 to 8.2 mg/g (median content of 5.5 mg/g, Fig. 2). In these samples, K and Fe presented intermediate concentrations with values between 14.9 and 26.8 mg/g, and between 4.0 and 27.5 mg/g, respectively (median content of 23.2 and 16.9 mg/g, respectively; Fig. 2), whereas the trends of trace elements were the same as in soils. Mn presented the highest concentrations and scattering, ranging from 0 to 1.65 mg/g (median content of 0.24 mg/g; Fig. 2). Sr was the least abundant varying from 0.06 to 0.13 mg/g (median content of 0.08 mg/g; Fig. 2) and Rb ranged from 0.11 to 0.16 (median content of 0.13 mg/g; Fig. 2).

In 2018, concentrations were generally lower but in quite the same trends as observed in the 2017 campaign. Ca again presented the highest concentrations, between 1.5 and 82.7 mg/g (median content of 9.4 mg/g; Fig. 2), Ti was again the least abundant, with concentrations between 0.4 and 6.6 mg/g (median content of 1.9 mg/g; Fig. 2), while K and Fe ranged between 14.4 and 26.7 mg/g, and between 2.5 and 37.4 mg/g, respectively with a median content of 19.0 and 9.2 mg/g, respectively (Fig. 2). Among the three trace elements, the concentrations of Mn were still the highest and the most widely scattered, varying from 0.02 to 0.43 mg/g (median content of 0.11 mg/g; Fig. 2). The lowest concentrations were again found in Sr, with between 0.042 and 0.11 mg/g (median content of 0.075 mg/g; Fig. 2), while the concentrations of Rb remained moderate, ranging between 0.073 and 0.13 mg/g (median content of 0.11 mg/g, Fig. 2).

3.2 Mineralogical composition

All the samples are made of quartz, albite and orthoclase, which is consistent with the geological context in the catchment (e.g. fluvial deposits and sands). Smectite is found in all samples with the exception of one topsoil sample (S7; Table 3) and one BLS sample, collected downstream the Beulie pond (BLS-6; Table 3). Calcite and kaolinite are not evidenced in the soil profiles, but appear in the composition of BLS samples (BLS-1 and 6b, respectively; Table 3). These two BLS samples were collected close to artificial drainage discharges into the watercourse of the Egoutier stream (Fig. 1). A very low presence of micas or illite was suspected in the BLS sample analyzed with the Thermo-Electron diffractometer (BLS-1 collected in 2017) but given the overlapping of their peaks, the discrimination of their type could not be characterized. In the other samples, the presence of micas was not evidenced but small amounts could be hidden behind other mineral peaks. No difference was observed between the two years of sampling for any of the BLS samples except for sample BLS-1 in which kaolinite was only detected in 2017 (Table 3).

Table3: Observed mineral species in selected samples of soil profiles and BLS (X: presence)

Soil profiles	***horizons or year of***	**Quartz**	**Calcite**	**Albite**	**Orthoclase**	**Smectite**	**Kaolinite**

/ BLS samples	***campaign***						
S2	A (topsoil)	*X*		*X*	*X*	*X*	
	C (subsoil)	*X*		*X*	*X*	*X*	
S7	A (topsoil)	*X*		*X*	*X*		
	C (subsoil)	*X*		*X*	*X*	*X*	
1	2017	*X*		*X*	*X*	*X*	*X*
	2018	*X*		*X*	*X*	*X*	
6	2017	*X*		*X*	*X*		
	2018	*X*		*X*	*X*		
6b	2017	*X*	*X*	*X*	*X*	*X*	
	2018	*X*	*X*	*X*	*X*	*X*	

255

256 *3.3 Particle size characteristics*

257 In topsoils, the grain-size classes 2-63 µm (silt) and 200-1600 µm (medium to coarse sands) presented
258 the highest proportions and dispersion varied from 26 to 56 % and from 24 to 51 %, respectively
259 (average percentages of 38 and 37 %, respectively; Fig. 3). The clay size fraction (0-2 µm) was the
260 lowest ranging between 0 to 3 % (average percentage equal to 2 %; Fig. 3). 63-200 µm (fine sands)
261 particle size fraction presented intermediate proportions ranging between 18 and 30 % (average
262 percentage of 23 %; Fig. 3). Despite high proportions of the silt size fraction, most topsoils were
263 mainly made of coarse particles ≥ 63 µm in size. Only topsoils S3 and S10 had a major contribution of
264 fine particles (< 63 µm; Fig. 3).

Subsoils presented different trends. The grain-size class 2-63 µm (silt) had the highest and the most dispersed values, varying from 29 to 78 % (average percentage of 50 %; Fig. 3). Despite higher proportions than in topsoils, the clay size fraction (0-2 µm) was still the least abundant, ranging between 1 and 8 % (average percentage of 3 %; Fig. 3). Coarser grain-size classes 63-200 and 200-1600 µm ranged from 10 to 28 % and from 9 to 51 %, respectively (average percentages of 20 and 27 %, respectively; Fig. 3). Subsoils were also mainly made of fine particles (< 63 µm) except for soils S5, S10, S11 and S12 which presented a major contribution of coarse particles (> 63 µm; Fig. 3).

Particle size distributions in BLS showed different trends. In 2017, the grain-size classes 2-63 µm (silt) and 200-1600 µm (medium to coarse sands) presented the highest proportions and dispersion varying from 16 to 79 % and from 1 to 73 %, respectively (average percentage of 42 and 35 %, respectively; Fig. 3). Proportions of the clay size fraction (0-2 µm) ranged between 1 and 12 % (average percentage of 4 %; Fig. 3). The grain-size class 63-250 µm (fine sands) showed an intermediate range between 6 and 35 % (average percentage of 19 %; Fig. 3). Textural characteristics were very variable in BLS depending on the location of the samples in the watercourse and no systematic composition of fine (< 63 µm) or coarse particles (> 63 µm) appeared in a BLS sample set.

[Figure 3]

Figure 3: Proportion of the size fractions in (a) the topsoils, (b) the subsoils, (c) the bed-load sediments (BLS) of 2017 and (d) the bed-load sediments (BLS) of 2018. The typology of each soil is mentioned in figure 1.

The sample set dating from 2018 was coarser. The highest contributions were only observed in the grain-size class 250-1600 µm, ranging between 27 and 89 % (average percentage of 65 %; Fig. 3). The clay size fraction was the least abundant, varying between 0 and 1 % (average percentage of 0.1 %; Fig. 3), and was even absent in some samples in the upstream part of the watercourse and at the outlet (BLS-2, 3, 4 and 7, respectively; Fig. 3). Despite a high dispersion, medium proportions of the

intermediate grain-size classes 2-63 µm and 63-250 µm were found, ranging from 6 to 43 % and from 4 to 49 %, respectively (average percentages of 18 and 16 %, respectively; Fig. 3).

4. Discussion

4.1 Vertical textural and geochemical soil variabilities: a weathering effect ?

4.1.1 Test of the bedrock uniformity

The presence of quartz, feldspar and clay minerals identified in soil samples (Table 3) is consistent with eroded material from granitic formations. Besides, SSC (i.e. Sologne Sands and Clays) and OS (i.e. Orleanais Sands) are ancient alluvia of the Loire River and thus correspond to detritic sediments resulting from the erosion of bedrocks from the Massif Central (Soucémarianadin and Verbèque, 2007). The fluvial origin of those bedrocks however involves a potential spatial heterogeneity in their deposits, particularly in the case of SSC (Soucémarianadin and Verbèque, 2007).

Soil chemical composition is driven by bedrock sources and weathering processes (Négrel et al., 2018b). To investigate elemental behavior during weathering at the catchment scale, potential bedrock heterogeinities should not be sources of textural and geochemical variabilities within soil profiles. Bedrock uniformity can be demonstrated by homogeneous rock sources. Ternary diagrams of major and trace elements with highly similar geochemical properties, against an insoluble one, were therefore plotted with bedrocks and Continental Crust compositions according to Parker, 1967.

K and Ca are soluble major elements concentrated in different mineral phases and with different geochemical behaviors. By being mainly hosted in K-feldspar (Beaucaire and Michard, 1982), K can trace silicate weathering (Négrel et al., 2018a). Ca is concentrated in plagioclases and K-feldspar (Beaucaire and Michard, 1982) and is highly mobile (De Vos et al., 2006). These elements were thus plotted with Ti contents, a weathering resistant element (Cornu et al., 1999), to trace detrital phase rock sources and the weathering effects. Ti and K contents in soil samples were distributed between granite and shist end-members (Fig. 4) suggesting different contributions from the Loire

River alluvial formations. These variations can, however, be the result of weathering as soil samples showed Ca losses compared to bedrock sources, implying Ca leaching (Fig. 4). The weathering of chemical elements within soil profiles results in the concentration of Ti in weathering products, because of its resistance to those processes (Milnes and Fitzpatrick, 1989). No significant differentiation was observed between topsoil and subsoil samples (Fig. 4), highlighting low weathering rates. Moreover, K mobility can be affected by different processes such as plant uptake (Kuhlmann et al., 1985) and release (Laskowski et al., 1995), and/or affinity with secondary clay minerals (Négrel et al., 2018a). In this context, the spread towards schist parent material (Fig. 4) can be explained by heterogeneities in the spatial weathering effects. These variabilities can be linked to different weathering rates according to soil type and/or different biological weathering depending on land cover. Since K and Ca play a role in plant biological cycles (Boyle and Voigt, 1973; Poszwa et al., 2000;), their contents clearly showed different migration trends between topsoil and subsoil samples depending on land cover (Fig. 4).

The same ternary diagram was constructed with trace elements (Rb and Sr) having similar behaviors to those of K and Ca during geochemical processes (Huntley and Hancock, 2001; Kabata-Pendias and Pendias, 2001; Négrel et al., 2018a). As in the first diagram Ti contents showed enrichment compared to bedrock compositions and no significant differences between topsoil and subsoil samples (Fig. 4), evidencing low weathering rates. Sr and Rb showed the same ranges in granite and in subsoil samples but enrichment and depletion, respectively, in topsoil. However, this suggests quite different cycles to those of K and Ca. Rb losses in topsoil could be the result of strong incorporation in secondary clay minerals (Négrel et al., 2018a) that are present in higher proportions in subsoil samples (*3.3*, Fig. 3). Despite being a plant nutrient, Rb migration presented similar trends according to land cover type, possibly linked to the low remobilization of its bound mineral (Kuhlmann et al., 1985). Sr is assumed to be removed at the same rates as Ca during weathering but is preferentially incorporated in clay minerals (Nesbitt et al., 1980). Moreover its release from detrital feldspar is slow (De Vos et al., 2006) and it can be strongly fixed in organic matter (Kabata-Pendias

and Pendias, 2001). These factors can explain the good differentiation between topsoil and subsoil samples and confirm that geochemical variations resulted from weathering processes.

[Figure 4]

Figure 4: Major (Ca, K, Ti) and trace elements (Rb, Sr) signatures of the soil investigated compared to bedrock and Continental Crust (CC) compositions according to Parker, 1967

Both diagrams show a principal granitic source (Fig. 4), corresponding to the soil mineralogical composition (*3.2*, Tab. 2) and to the geological bedrock signature of the upstream part of the Loire River catchment area. Ti enrichments highlight low weathering rates and Ca, K, Rb and Sr dispersion shows different behaviors associated with the biological cycle of nutrients and weathering. It suggests low lateral variabilities but the absence of vertical ones created by bedrock heterogeneities.

4.1.2 Homogeneity of the soil characteristics

The catchment area is mainly covered by neutral Redoxisol (Soucémarianadin and Verbèque, 2007) characterized by hydromorphic conditions because low permeabilities are observed in the subsoil leading to the presence of a temporary perched water table (Baize et al., 2009). Water table variations within soil profiles imply redox reactions modifying soil components mobility (Favrot and Vizier, 1994). Moreover, clays (particles < 63µm) are subjected to illuviation processes from topsoil to subsoil layers (Pollet, 2009).

To confirm that soil geochemical variations reflect soil weathering, we investigated the Ti contents because Ti-bearing minerals are frequently found in sedimentary rocks as detrital phases resulting from erosion of magmatic rocks (Milnes and Fitzpatrick, 1989). Moreover, because Ti resists weathering, Ti content is used to understand soil genesis (Kabata-Pendias and Pendias, 2001) and to estimate the degree of weathering (Cornu et al., 1999). In our case, mean Ti content was 6.4 mg/g (Fig. 5), which is a slightly higher than but in the same order of magnitude as the median content measured in European top- and subsoil layers (5.7 mg/g; De Vos et al., 2006). Likewise, Ti content ratios between topsoil and subsoil were similar between soil profiles developed on SSC (i.e. Sologne

Sands and Clays, *[Ti] topsoil / [Ti] subsoil* ratio of 1.03, Fig. 5) and European soils (equals to 1.02; De Vos et al., 2006; Reimann et al., 2014a; Reimann et al., 2014b). Lower enrichments of Ti in topsoils are therefore consistent with a slow weathering of these soils. Conversely, profiles developed on OS (i.e. Orleanais Sands) had a mean *[Ti] topsoil / [Ti] subsoil* ratio of 0.95 (Fig. 5), due to higher concentrations of Ti in the suboil, already demonstrated by Larue and Etienne (2000) who documented higher Ti contents in OS than in SSC. Following Reimann and De Caritat (2000), this difference can lead to Ti-rich "geogenic" dust in deeper soil horizons. Furthermore, the depth at which the subsoil occurred was deeper in OS (from 48 to 90 cm with a mean value of 71 cm) than in SSC (from 22 to 65 cm with a mean value of 39 cm). This greater depth of the OS soil profiles could thus balance the enrichment of Ti in topsoil layers. In spite of different bedrock signatures, Ti contents at the Egoutier scale showed low variability and were quite similar in all soil profiles.

[Figure 5]

Figure 5: Proportions of titanium in top- and subsoils developed on (a) Sologne sands and clays (SSC) and (b) Orleanais sands (OS). Differences in fine grain-size fraction proportions between top- and subsoils

In Redoxisol profiles, clay contents derive from pre-existing minerals but the weathering of initial minerals is far from complete (Righi and Meunier, 1995). Montmorillonite-type smectite is for instance a secondary mineral formed by the weathering of feldspar in neutral to alkaline conditions where poor drainage occurs (Pickering, 1986). The clay contents in topsoil and subsoil samples (illustrated by the *0-63 µm subsoil / 0-63 µm topsoil* ratio, Fig. 5) can therefore highlight heterogeneities inherited from the underlying fluvial deposits or the degree of soil weathering. Depending on the soil types investigated, three trends of the *0-63 µm topsoil / 0-63 µm subsoil* ratio were observed (Fig. 5). The Redoxisol *0-63 µm topsoil / 0-63 µm subsoil* ratio ranged between 1.00 and 1.73 (mean value of 1.39, Fig. 5). The Planosol *0-63 µm topsoil / 0-63 µm subsoil* ratio was the highest with a mean value of 1.83 and the Brunisol one was the lowest, at 0.51 (Fig. 5). These results suggest both low weathering and illuviation processes, and low heterogeneities in the clay contents within Redoxisol profiles but an enrichment in clays in subsoil and in topsoil within the Planosol and

Brunisol ones, respectively (Fig. 5). These observations are consistent with the vertical dynamic of these types of soils: although Planosol and Brunisol are both hydromorphic, Planosols are characterized by high textural differentiation while Brunisols are not (Baize et al., 2009). In this context, the smectite (Table 3) was formed by the weathering of primary minerals and the soil vertical dynamics controls its migration from topsoil to subsoil layers.

Given the uniformity of bedrocks and the processes influencing the soil characteristics (*4.1*), it can be concluded that the different textural and geochemical characteristics of the soils evidence the effects of homogeneous low weathering rates at the catchment scale.

4.2 Geochemical signature of the weathering processes

4.2.1 Factors having an impact on soil geochemistry

Pedogenesis starts with bedrock alteration, but climate, soil organisms, vegetation and time distinguish the different horizons with specific geochemical signatures (Sucharovà et al., 2012). The first principal component of the PCA explained 40 % of the total variance, the second 30 % and the third one, only 10 %. Around 70 % of the signal distribution was thus explained by two principal directions (Fig. 6). The first one results from K and Fe distribution while the second only from Ca and Rb distribution (Table 2). The PCA was therefore considered as being representative with two principal directions which were enough to explain the observed variations between top- and subsoil layers. Moreover, despite showing a high variability, PCA results support observations already made (see §*4.1*).

Three main behaviors were identified. K, Sr and Ti were not specific to topsoil or subsoil samples, suggesting homogeneity of those elements at the profile scale, whereas Ca, Rb and Fe were only found in subsoil samples. On the contrary, Mn presented a specificity to topsoil layers (Fig. 6).

Compared to European soil signatures (De Vos et al., 2006), K (topsoil set), Ti and Fe (subsoil set) contents were similar. However, the investigated soils were less concentrated in K (subsoil samples), Sr, Ca, Fe (topsoil set) and Mn, but richer in Rb.

K and Sr contents seem to be influenced by the same phenomena (Fig. 6) and these differences with European trends could be due to low weathering rates, few interactions with secondary minerals and/or a mineral phase effect, rather than to lithology effects. Indeed, the mineralogical composition (quartz, albite, orthoclase and smectite) of the soil horizons does not vary according to soil type, land cover and/or bedrock. However, as seen in part *4.1.2*, Ti presented an independent behavior influenced by bedrock types (Fig. 6), which could explain the higher concentrations than in European soils.

Rb, Fe and Mn were not influenced by soil type, bedrock or land cover type, while Ca seemed to be linked with the latter (Fig. 6). Given the geological context of the Egoutier catchment, calcite and plagioclase are the two main bearing phases of Ca (Négrel and Grosbois, 1999) and low contents of Ca could therefore be partly explained by the virtual absence of calcite at the catchment scale (Table 3). Ca is highly soluble (De Vos et al., 2006), mostly under low pH conditions (Bailey et al., 1996). Topsoils pH values ranged between 6.5 and 8.3 (median value of 7.1, Soucémarianadin and Verbèque, 2007) suggesting than Ca leaching was not the main process involve in its distribution. Ca is a crucial element for the mineral nutrition of trees (Drouet and Herbauts, 2008) and this could explain why Ca was mainly representative of subsoil samples and influenced by land cover types (Fig. 6). Rb is mainly hosted by K-feldspar (Beaucaire and Michard, 1982) and shows strong affinity with clay minerals after weathering (Négrel et al., 2018a). Higher trends than European soils can thus be linked with the granitic sources of the fluvial bedrocks providing high supplies in K-feldspar and sandy-clay soils offering high stocks of secondary minerals. Regarding Fe, its depletion in topsoil compared to the European soils can be caused by its high mobility in Redoxisol because of redox reactions (Pollet, 2009). Dissimilarities in Mn contents can be correlated with the mineralogical and physicochemical characteristics of the investigated soils.

[Figure 6]

Figure 6: PCA of the geochemistry and characteristics of the soil horizons

Surprisingly, couples of chemical elements known to follow the same trends during weathering, biochemical and redox processes, such as Ca/Sr (Bailey et al., 1996), K/Rb (Huntley and

Hancock, 2001) and Fe/Mn (Kabata-Pendias and Pendias, 2001) were not observed. In our case, the observed chemical elements distribution was mainly driven by parent mineral composition, weathering resistance, potential interaction with secondary phases, or the inherent dynamic of hydromorphic sandy-clay soils, leading to these dissimilarities. Only Ca, and particularly Ti were slightly influenced by study-case parameters, such as land cover and bedrock.

4.2.2 Behavior of the chemical elements in the soil profiles

Numerous chemical processes occur during weathering: dissolution, hydration, hydrolysis, oxidation, reduction and carbonatization (Kabata-Pendias and Pendias, 2001), implying changes in mineral chemical composition by the leaching of alkaline/alkaline earth cations. Parent minerals therefore tend to disappear depending on their weathering resistance, while secondary ones are created (Oludare, 2017). Comparing soil elemental composition with the parent material, Kabata-Pendias and Pendias (2001) highlighted element mobility during pedogenic processes. As bedrock was not sampled during the present survey, the geochemistry of one selected subsoil was taken as representative of the local geochemical background. The S8 profile subsoil layer (Fig. 1) was thus chosen since its composition was representative of all soil profiles. The enrichment factors (EF, Eq. 1) were therefore calculated both using S8 composition as a reference, and considering Ti as a conservative element. EF should be used with caution since the behavior and weathering of some chemical elements in soil profiles can reflect fractionation through uptake by plants, bonded to organic material or forming new minerals (Sucharovà et al., 2012). For instance, Reimann and Caritat (2000) suggested that EF mainly reflect the relative solubility of elements. In this study, EF were therefore considered as reflecting both the fractionation and continuity of near-surface processes: weathering and erosion. To visualize general elemental behaviors at catchment scale, boxplots of calculated EF were constructed (Fig. 7). To distinguish retention, fractionation or illuviation processes causing these observations, elemental contents were normalized to fine grain-size particles (0-63 µm) as follows:

$$[El]_{Norm} = [El]_{sample} / (0 - 63\ \mu m) \qquad \text{Eq. 2}$$

With $[El]_{sample}$ the elemental concentration of each sample in µg/g and (0 – 63 µm) the percentage of this grain-size fraction. Normalized contents were represented as binary plots (Fig. 8). Given the uncertainties on micas low presence and type, their potential role in the geochemical effects of weathering is not discussed. Three behaviors were distinguished in topsoil layers (Fig. 7).

K and Sr presented a mean EF of 1.1 (Fig. 7), confirming no enrichment in topsoil layers, which is consistent with European trends (De Vos et al., 2006; Reimann et al., 2014a; Reimann et al., 2014b). K and Sr are highly mobile elements (De Vos et al., 2006) whose main parent minerals are different: K-feldspar for K (Négrel and Grosbois, 1999) and plagioclase and K-feldspar for Sr (Blum and Erel, 1997), respectively. K-feldspars are more resistant than plagioclases to weathering processes (Goldich, 1938) but Sr release from detrital feldspars is a slow process (De Vos et al., 2006). Even if Sr is known to be incorporated in clay minerals (Kabata-Pendias and Pendias, 2001), cations with low hydration energy, such as K^+, are preferentially fixed by clays (Sawhney, 1972). Despite that, preferential incorporation of K in subsoil clay minerals can be balanced by high rates of K released in topsoil layers by decomposing leaf litters (Laskowski et al., 1995). Similarly, Sr mobility can be limited by its strong interaction with organic matter mainly contained in topsoils (Kabata-Pendias and Pendias, 2001). K and Sr normalized contents were linear and showed similar evolutions (Fig. 8). Nevertheless, a phase effect illustrates their interaction with clay minerals in subsoil layers (Fig. 8).

Fe, Ca and Rb presented mean EF lower than 1 (Fig. 7), illustrating a depletion of these elements in topsoil samples, also consistent with European trends, except for Rb (De Vos et al., 2006; Reimann et al., 2014a; Reimann et al., 2014b). On the one hand, results reflected the effect of redox reactions on Fe vertical distribution (Favrot and Vizier, 1994) and its strong interactions with clay minerals (Pollet, 2009). Indeed, in spite of the weak mobility of Fe (Négrel and Deschamps, 1996), its solubility is favored in saturated hydromorphic soils, as is its precipitation as oxi/hydroxydes and/or its adsorption on clay minerals (Kabata-Pendias and Pendias, 2001), mostly located in subsoil layers (Fig. 3). Fe normalized contents evidenced a low differentiation between topsoil and subsoil layers (Fig. 8) confirming the combination of secondary minerals precipitation and its adsorption on clays. On the other hand, the results plotted in Fig. 7 demonstrate Ca and Rb leaching by weathering of their

primary minerals. The high variability of EF for Ca (Fig. 7) can be explained by different mean values according to land cover types: 0.28 in topsoil layers under coniferous forests, 0.42 in those under hardwood forests, and 1.15 in those under agricultural parcels.These differences suggest liming of agricultural parcels given the importance of Ca for soil exchange complexes (Drouet and Herbauts, 2008), favouring nutrient availability (Holland et al., 2018). Furthermore, Ca leaching appeared higher in topsoil layers under coniferous forests which might be the result of a typical soil acidification (Hornung, 1985). Nevertheless, normalization demonstrates a matrix effect responsible for higher contents in subsoil layers (Fig. 8). Negatively-charged clay surfaces can adsorb divalent ions more strongly than monovalent ones (De Vos et al., 2006). The distribution of Ca is thus also driven by interactions with secondary phases. Rb distribution is driven by a combination of unaltered K-feldspars in topsoil, highlighted by K distribution, and illuviation of clay minerals to subsoil layers confirmed by the absence of phase effect after normalization (Fig. 8). This could elucidate the difference with European top-/subsoil ratios where a constant Rb content is observed at profile scale (De Vos et al., 2006).

Mn presented a mean EF of 3.3, demonstrating a high enrichment in topsoil layers. This is consistent with previous results but not with constant European trends (De Vos et al., 2006). Soluble and exchangeable, Mn^{2+} are dominant cations under strongly acidic conditions, and are immobilized in neutral to basic soils (Adam and Beaugelin-Seiller, 2005; De Vos et al., 2006). The soil profiles in the Egoutier catchment have a mean pH value of 7.35 (Soucémarianadin and Verbèque, 2007), Mn could thus form insoluble oxides under oxidizing conditions (De Vos et al., 2006), which cannot be destabilized afterwards. It could explain the difference with the Fe pattern. Moreover, normalization with fine grain-size particles (0-63 µm, Eq. 2) highlighted low differences between topsoil and subsoil layers concentrations (Fig. 8), suggesting a behavior slightly influenced by phase effects.

[Figure 7]

Figure 7: Enrichment factors (EF) calculated for topsoil samples and for the two bed-load sediment (BLS) sample sets dating from 2017 and 2018

Weathering processes have variable consequences with respect to local climate, mineralogic and pedogenic characteristics of the studied site. Moreover, the element distribution demonstrated different influencing factors. Some elements presented low mobility because of biological supplies (K) or immobilization by redox reactions (Mn) and organic matter fixation (Sr), while others showed high mobility induced by high leaching rates (Fe, Ca, Rb) enhanced by redox reactions (Fe), illuviation processes (Rb) and soil acidification (Ca). In spite of low weathering rates and variable mobilities, all the investigated elements are at least slightly subjected to leaching processes and interactions with secondary mineral phases, except strongly immobilized ones.

4.3 Geochemical impact of erosion processes

4.3.1 Behavior of the geochemical elements in the bed-load sediment

Suspended particulate matter carried by streams and rivers is the result of rock and soil erosion processes. Particles are therefore composed of selected resistant primary minerals and secondary phases, controlling the transport and deposition dynamics of associated elements over continental areas (Viers et al., 2009) and controlling the behaviors of these elements in the sedimentary cycle (Nesbitt et al., 1980). Grain size distribution and elemental sediment contents (Defersha and Melesse, 2012) represent two key parameters to decipher these kinds of patterns. To visualize erosion effects on elemental behaviors at catchment scale, boxplots of bed-load sediments EF were compared to topsoil ones (Fig. 7). Moreover to distinguish selective erosion, transport or deposition processes causing these observations, elemental contents normalized to fine grain-size particles (0-63 µm, Eq. 2) were represented as binary plots (Fig. 8).

Firstly, all the investigated elements except for Mn presented higher EF in BLS than in topsoil layers (Fig. 7).

Mn contents were similar in topsoil, in BLS and in subsoil layers after normalization (Fig. 8), evidencing a behavior resulting from phase effects. Mn lower enrichments in BLS are therefore due to dilution by other mineral phase supplies. Ghadiri and Rose (1991) demonstrated that eroded sediments

generally present higher contents in chemical elements than soils. Erosion processes can destabilize aggregates in soils, but aggregates can also be formed directly in streams. However, the proportions of this second type of aggregate appear to be less (Ghadiri and Rose, 1991). Higher EF for Fe, K, Ca, Rb and Sr in BLS could imply, for instance, a phase effect by selective erosion of secondary clay minerals as these minerals fixed the weathered chemical elements and are preferentially transported by runoff. However, that does not explain the large enrichments in Ca. Higher BLS contents could also be linked with a preferential deposit of coarser particles (Fig. 3) made of K-feldspars and plagioclases (Tab. 2), rich in K, Rb and Ca, Sr, respectively. Although clay minerals are more prone to be exported by erosion, the transport of other mineral phases can be facilitated by break-up processes (Anderson et al., 2007) and a matrix effect should also be considered as it changes the mineral phases composing each particle size fractions.

Secondly, all the chemical elements except Fe presented mean EF higher than 1 in BLS compared to subsoil layers (Fig. 7). Apart from K, these results are consistent with European stream sediments (De Vos et al., 2006). K and Sr followed similar dynamics with mean EF of 2.6 and 2.4 in 2017, 5.8 and 5.4 in 2018, respectively (Fig. 7) testifying to K and Sr contents in BLS and higher inputs in 2018. Besides, Négrel (1999), demonstrated that Sr is subject to depletion in sediments because of the presence of K-feldspars, but Sr contents can also be caused by detrital feldspars (De Vos et al., 2006). Moreover, K and Sr associated with both unaltered feldspars and clay minerals seem to have the same sensitivity to erosion. While no phase effect was observed between the two years of sampling, K and Sr demonstrated different BLS particle sizes. The difference observed with European soils for K contents could therefore be explained both by low weathering rates and high feldspar content within the Egoutier catchment.

The Rb behavior in BLS was similar to that of K and Sr but enrichments were lower with mean EF of 1.1 and 2.3 in 2017 and 2018, respectively (Fig. 7). The same Rb contents in BLS and in topsoil in 2017 after normalization (Fig. 8) evidenced its enrichment in sediments by a selective erosion of clay minerals. Moreover, Négrel and Deschamps (1996) observed Rb depletion in sediments compared to the average contents of basaltic parent rocks while Négrel (1999) observed Rb

enrichment in sediments compared to the average contents of granitic parent rocks. The Rb mean EF close to 1 in 2017 (Fig. 7) and the same evolution for K suggest the contribution of additionnal topsoil layers supplied by almost unaltered K-feldspar from the erosion of granitic bedrocks.

[Figure 8]

Figure 8: Evolution of the chemical elements between soils and bed-load sediments (BLS) normalized by fine grain-size particles (0-63 µm, Eq. 2)

Fe enrichments in BLS remained below 1 (mean EF of 0.9 and 0.5, respectively, Fig. 7) suggesting its depletion in BLS compared to subsoil layers. Indeed, lower Fe contents in sediments were already demonstrated by Négrel (1999) and seem to be caused by higher proportions of K-feldspar. Despite the selective erosion of clay minerals, leading to higher enrichments in BLS than in topsoil (Fig. 7), the dilution of Fe contents suggests that topsoil layers are the main contributors to BLS.

Ca presented very high enrichments in BLS with mean EF of 9.2 in 2017 and 16.2 in 2018, respectively (Fig. 7). These values are surprising given the absence of carbonaceous phases (Table 3) and the leaching of this element in soils. The highest enrichments were observed on the release of rainwaters from anthropized areas (sample 6b) and of the PH sewage waters (sample 3), respectively. These enrichments could therefore be due to anthropogenic supplies, and more particularly to runoff on artificial surfaces made of calcareous gravels. Besides, calcite was observed in sample 6b (Table 3).

Natural fractionation of the investigated elements appears to be driven both by weathering and erosion. The combination of these two processes was moreover already demonstrated by Reimann and De Caritat (2005). On the one hand, erosion induced variations of the mineral phases occurring in each grain-size fraction, except for highly insoluble minerals; on the other hand, supplying layers and selective erosion explained variations in element contents (K, Sr, Rb and Fe). Other elements, such as Mn, seem to remain independent from preferential erosion: diluted in BLS (Mn), or artificially added by the runoff on anthropized areas (Ca).

603 4.3.2 Annual variability of bed-load sediment geochemistry

604 Erosion and deposition processes depend on numerous local factors such as rainfall intensity,
605 infiltration, runoff rates, soil properties and soil surface conditions (Defersha and Melesse, 2012).
606 These factors differed throughout the two years of sampling, especially the amount of rain. Only 0.8
607 mm of rain fell 48 hours before the field campaign in 2017, while 7.3 mm fell before the 2018
608 campaign. This difference enables visualization of erosion rates, potential selectivity as well as
609 transportation and deposition variabilities at low temporal scales to be visualized. To evidence the
610 geochemical influence and spatial variabilities of rain amounts, binary plots with the enrichment
611 factors (EF) of elements with different observed behaviors were constructed (Fig. 9).

612 [Figure 9]

613 *Figure 9: Evolution of geochemical enrichment factors (EF) between 2017 and 2018 bed-load sediment (BLS) sample sets*

614 Globally, no difference was observed for Mn mean enrichments between the 2017 and 2018
615 sample sets (Fig. 7), demonstrating quite similar supplies in Mn oxides during erosion, as topsoil
616 layers were the main source of BLS. However, this observation depends on rainwater flow paths, as
617 shown by the spatial evolution of Mn EF: all the samples presented increasing EF in 2018 except those
618 collected at sewage and stormwater outfalls (BLS-1, 3, 5 and 6b, Fig. 9). Topsoil supplies to BLS were
619 thus locally diluted where runoff from urban areas contributed. The Mn geochemical signature thus
620 appeared constant at catchment scale but was mainly driven by topsoil contributions to BLS, which
621 were highly dependent on permeable areas.

622 Contrary to Mn, EF calculated for the 2018 sample set were always higher for all the other
623 elements investigated (Fig. 7 and 9), highlighting the strong covariation between element contents and
624 rainfall amounts.

625 The mean EF for K and Sr were more than twice as high in BLS dating from 2018 than those
626 from 2017 (Fig. 7), evidencing higher inputs. Samples collected in 2018 presented a coarser
627 composition (Fig. 3), confirming higher feldspar erosion rates and deposition. Moreover, these
628 differences were not linked with a potential phase effect (Fig. 8) supporting K and Sr incorporation in

different mineral phases and break-up processes explaining their presence in all grain-size fractions. Nonetheless, K EF spatial evolution showed the highest increases where fewer fine grain-size particles deposited (BLS-2, 3, 4 and 7, Fig. 9 and 3), suggesting influence of longer fine particle (< 63 µm) transportation distances in 2018. Likewise, 2018 Sr EF decreased only on both sides of the pond (BLS-5 and 6, Fig. 9), where the proportions of fine grain-size particles declined the least (Fig. 3).

The Rb evolution in BLS was quite similar but lower than K and Sr, with mean EF that were twice as high in 2018 as in 2017 (Fig. 7). Strongly incorporated in K-feldspar as in clay minerals, the 2018 increase was due to enhanced particle supplies and selective erosion of clay. Its presence in the two mineral phases is evidenced by well differentiated Rb contents between topsoil and subsoil layers, not resulting from higher contents of clay minerals (Fig. 8). Moreover, its spatial evolution was quite similar to that of K and Sr ones, with the highest increases in the coarser samples of 2018 (BLS-2, 3, 4 and 7, Fig. 9). EF for Rb in 2018 may thus evidence the contribution of subsoil layers and coarser deposits in transportation zones because of higher rainfall.

Fe presented a higher EF in 2018 than in 2017, both locally (Fig. 9) and at catchment scale (Fig. 7), but the increase was lower than that of Rb. Fe is mainly hosted by clay minerals from subsoil layers. Like Rb, 2018 enrichments could be the result of selective erosion of clay minerals combined to higher contributions from the Fe-rich layer as 2018 BLS had a coarser composition (Fig. 3) and Fe dynamic was not due to phase effects (Fig. 8).

Ca behaves similarly to Fe but the higher mean EF observed in 2018 is driven by a phase effect (Fig. 8), reflecting higher supplies by the runoff on anthropized areas due to rain amounts, and the concentration of Ca in one particular grain-size fraction. These effects are visible in the local evolution of Ca EF: samples collected from urban rainwater contributions presented a higher increase in Ca (BLS-1 and 3, Fig. 9) and in the coarser grain-size fraction (250-1600 µm, Fig. 3). This evolution was not observed in sample 6b, highlighting more transportation in 2018, as the highest increase in Ca was shown at the catchment outlet (Fig. 9).

The sediment geochemistry is also influenced by both depletion and the transportation/deposition dynamic of selected grain-size fractions and mineral phases. Therefore, rain amounts drive the supplying quantities but also the sources of particles within soil profiles and in the catchment. Deviations of each element from their mean EF (Fig. 7) evidence high deposition zones and input heterogeneities. These differences are linked with the pond and the impermeable urban areas for some elements (Mn, Ca).

5. Conclusions

Despite a bedrock fluvial origin and low chemical variations according to land cover and bedrock types, the small scale of the Egoutier catchment allows a good visualization of silicate weathering and erosion processes, as well as stream transportation and deposition dynamics. Enrichment factor (EF) calculation was a useful tool to understand both the fractionation and continuity of these near-surface processes as soil geochemical profiles were not well differentiated.

In the case of low weathering rates, except chemical elements that were strongly immobilized, because of redox reactions for example, most of the elements are only slighlty subjected to leaching. However, slow weathering enabled the identification of different forcing factors. Egoutier catchment hydromorphic soils are strongly controlled by redox reactions, but the main characteristic driving the specific elemental distribution within soil profiles is necessarily the weathering resistance of primary minerals. Combined to that, some characteristics, such as plant uptake and release, play ubiquitous roles, while others, such as illuviation processes or soil acidification, are site-dependent.

Influencing factors during erosion processes have more complex consequences. Firstly, as already known, a selection of depleted particles occurs favoring a prefential erosion of fine grain-sizes, such as clay minerals. However, modifications of mineral grain sizes through disaggregation or break-up processes can encourage the erosion of other mineral phases. Beyond that, the main factors controlling sediment geochemistry are erosion rates, particle sources, and stream

transportation/deposition dynamics. Logically, more depleted particles are supplied to sediments during periods of higher rainfall. This leads to higher enrichments in every chemical element except those mainly contained in topsoil, because subsoil layer particles also contribute to bed-load sediments (BLS) when soils are saturated and higher contributions of urban rainwaters buffered topsoil supplies to BLS. Moreover, longer transportation distances of fine grain-size particles lead to local enrichments of elements carried by coarser particles. Furthermore, caution must be taken concerning some elements which can be artificially supplied in this kind of peri-urban stream.

BLS geochemistry results thus from the combination of textural and mineralogical selectivity during erosion, but also from sources within soil profiles and waterflow equilibrium between deposition and transportation, which are directly dependent on the characteristics of rainfall events. Therefore, BLS EF scattering highlights different soil profile sensitivities to erosion and sedimentary dynamic variations along the watercourse. These observations provide useful information to understand and predict sediment behavior and associated geochemistry. It could therefore be interesting to conduct similar studies on suspended particle geochemistry correlated with more detailed pluviometric characteristics than just rain amounts. A better characterization will allow geochemical modeling to be applied to erosion processes and river particulate transportation. The peri-urban context of this watershed also allows the same application for the geochemistry of contaminants, supplied by sewage water inputs and urban stromwater runoff.

Acknowledgments

This work and the PhD grant of L. Ledieu were funded by the Région Centre Val de Loire (France) and are part of the Academic Initiative Project MOSAIC led by A. Simonneau. This work was also supported by a grant overseen by the French National Research Agency (ANR) as part of the "Investments d'Avenir" Programme LabEx VOLTAIRE, 10-LABX-0100. This study benefited from collaboration with the GéhCO laboratory and J-P. Bakyonoo is warmly thanked for his help during analysis. We are grateful to P. Penhoud for analytical and technical support in XRD analysis. L. Baude, H. Alphonse and S. Picault are thanked for the sampling authorization at the G. Daumézon hospital and in the town of Semoy. We acknowledge F. Romain and S. Valdelièvre for their support during the soil survey.

References

Anderson, S.P., Von Blanckenburg, F., White, A.F., 2007. Physical and Chemical Controls on the Critical Zone. Elements 3 No. 5, 315-319.

Bailey, S.W., Hornbeck, J.W., Driscoll, C.T., Gaudette H.E., 1996. Calcium inputs and transport in a base-poor forest ecosystem as interpreted by Sr isotopes. Water Resources Research 32 No. 3, 707-719.

Baize, D., Girard, M.C. Beaudou A.G., Poss R., 2009. Référentiel pédologique 2008. Quae, Versailles.

Barbieri, M., 2016. The Importance of Enrichment Factor (EF) and Geoaccumulation Index (Igeo) to Evaluate the Soil Contamination. Journal of Geology and Geophysics 5 No. 237, 1-4.

Barrows, H.L., Kilmer, V.J., 1963. Plant Nutrient Losses from Soils by Water Erosion. Advances in agronomy 15, 303-316.

Beaucaire, C., Michard, G., 1982. Origin of dissolved minor elements (Li, Rb, Sr, Ba) in superficial waters in a granitic area. Geochemical Journal 16 No. 5, 247-258.

Berger, G., Desprez, N., 1969. Carte de France (1/50 000), "Orléans (363)". BRGM, Orléans.

Bernasconi, S. M., Biglink Project Members, 2008. Weathering, soil formation and initial ecosystem evolution on a glacier forefield: a case study from the Damma Glacier, Switzerland. Mineralogical Magazine 72 No. 1, 19-22.

Blum, J.D., Erel, Y., 1997. Rb-Sr isotope systematics of a granitic soil chronosequence: The importance of biotite weathering. Geochimica et Cosmochimica Acta 61 No. 15, 3193-3204.

Bormann, F. H., Likens, G. E., 1967. Nutrient cycling. Science 155 No. 3761, 424-429.

Bowen, H.M., Dymond, J.A., 1955. Strontium and barium in plants and soils. Proceedings of the Royal Society of London. Series B-Biological Sciences 144 No. 916, 355-368.

Boyle, J. R., Voigt, G. K., 1973. Biological weathering of silicate minerals. Plant and Soil 38 No. 1, 191-201.

Brady, P. V., 1991. The effect of silicate weathering on global temperature and atmospheric CO2. Journal of Geophysical Research: Solid Earth 96 No. B11, 18101-18106.

Butt, C. R. M., 1992. Physical weathering and dispersion. In Handbook of Exploration Geochemistry 4, 97-113. Elsevier Science BV.

Cerdan, O., Le Bissonnais, Y., Couturier, A., Bourennane, H., Souchère, V., 2002. Rill erosion on cultivated hillslopes during two extreme rainfall events in Normandy, France. Soil & Tillage Research 67, 99-108.

Cleaves, E. T., Godfrey, A. E., Bricker, O. P., 1970. Geochemical balance of a small watershed and its geomorphic implications. Geological Society of America Bulletin 81 No. 10, 3015-3032.

Cornu, S., Lucas, Y., Lebon, E., Ambrosi, J.P., Luizão, F., Rouiller, J., Bonnay, M., Neal, C., 1999. Evidence of titanium mobility in soil profiles, Manaus, central Amazonia. Geoderma 91 No. 3-4, 281-295.

Cullers, R.L., Barrett, T., Carlson, R., Robinson, B., 1987. Rare-earth element and mineralogic changes in Holocene soil and stream sediment: a case study in the wet mountains, Colorado, U.S.A.. Chemical Geology 63, 275-297.

Cullers, R., 1988. Mineralogical and chemical changes of soil and stream sediment formed by intense weathering of the Danburg granite, Georgia, U.S.A.. Lithos 21, 301-314.

Delmas, M., Pak, L.T., Cerdan, O., Souchère, V., Le Bissonnais, Y., Couturier, A., Sorel, L., 2012. Erosion and sediment budget across scale: A case study in a catchment of the European loess belt. Journal of Hydrology 420, 255-263.

Defersha, M.B., Melesse, A.M., 2012. Effect of rainfall intensity, slope and antecedent moisture content on sediment concentration and sediment enrichment ratio. Catena 90, 47-52.

De Vos, W., Tarvainen, T., Salminen, R., Reeder, S., De Vivo, B., Demetriades, A., Pirc, S., Batista, M.J., Marsina, K., Ottesen, R.T., O'Connor, P.J., Bidovec, M., Lima, A., Siewers, U., Smith, B., Taylor, H., Shaw, R., Salpeteur, I., Gregorauskiene, V., Halamić, J., Slaninka, I., Lax, K., Gravesen, P., Birke, M., Breward, N., Ander, E.L., Jordan, G., Duris, M., Klein, P., Locutura, J., Bel-lan, A., Pasieczna, A., Lis, J., Mazreku, A., Gilucis, A., Heitzmann, P., Klaver, G., Petersell, V., 2006. Geochemical Atlas of Europe: Part 2: Interpretation of geochemical maps, additional tables, figures, maps, and related publications. Geological Survey of Finland.

Douglas, I., 2012. Peri-urban ecosystems and societies: Transitional zones and contrasting values. In The peri-urban interface, 41-52. Routledge.

Drouet, T., Herbauts, J., 2008. Evaluation of the mobility and discrimination of Ca, Sr and Ba in forest ecosystems: consequence on the use of alkaline-earth element ratios as tracers of Ca. Plant and soil, 302 No. 1-2, 105-124.

Emberson, R., Hovius, N., Galy, A., Marc, O., 2016. Chemical weathering in active mountain belts controlled by stochastic bedrock landsliding. Nature Geoscience 9 No. 1, 42.

Favrot, J., Vizier, J.F., 1995. Solums à caractères hydromorphes. Référentiel pédologique, 181-189.

Gaillardet, J., Dupré, B., Allègre, C. J., 1999. Geochemistry of large river suspended sediments: silicate weathering or recycling tracer?. Geochimica et Cosmochimica Acta, 63 No. 23-24, 4037-4051.

Ghadiri, H., Rose, C.W., 1991. Sorbed chemical transport in overland flow: II. Enrichment ratio variation with erosion processes. Journal of Environmental Quality 20 No. 3, 634-641.

Goldich, S.S., 1938. A study in rock-weathering. The Journal of Geology 46 No. 1, 17-58.

Grau, H.R., Hernandez, M.E., Gutierrez, J., Gasparri, N.I., Casavecchia, E.E., Flores-Ivaldi, E.E., Paolini, L., 2008. A Peri-Urban Neotropical Forest Transition and its Consequences for Environmental Services. Ecology and Society 13 No. 1.

Grosbois, C., Négrel, Ph., Fouillac, C., Grimaud, D., 2000. Dissolved load of the Loire River: chemical and isotopic characterization. Chemical Geology 170, 179-201.

Guo, L., Lin, H., 2016. Critical zone research and observatories: Current status and future perspectives. Vadose Zone Journal 15 No. 9.

Harriss, R. C., Adams, J. A., 1966. Geochemical and mineralogical studies on the weathering of granitic rocks. American Journal of Science 264 No. 2, 146-173.

Heindel, R.C., Lyons, W.B., Welch, S.A., Spickard, A.M., Virginia, R.A., 2018. Biogeochemical weathering of soil apatite grains in the McMurdo Dry Valleys, Antarctica. Geoderma 320, 136-145.

Holland, J. E., Bennett, A. E., Newton, A. C., White, P. J., McKenzie, B. M., George, T. S., Pakeman, R. J., Bailey, J. S., Fornara, D. A., Hayes, R. C., 2018. Liming impacts on soils, crops and biodiversity in the UK: a review. Science of the Total Environment 610, 316-332.

Hornung, M., 1985. Acidification of soils by trees and forests. Soil use and management 1 No. 1, 24-27.

Huntley, D.J., Hancock, R.G.V., 2001. The Rb contents of the K-feldspar grains being measured in optical dating. Ancient TL 19 No. 2, 43-46.

Johnson, C. C., Ander, E. L., 2008. Urban geochemical mapping studies: how and why we do them. Environmental Geochemistry and Health 30 No. 6, 511.

Johnson, N. M., Likens, G. E., Bormann, F. H., Pierce, R. S., 1968. Rate of chemical weathering of silicate minerals in New Hampshire. Geochimica et Cosmochimica Acta 32 No. 5, 531-545.

Kabata-Pendias, A., Pendias, H., 2001. Trace Elements in Soils and Plants. CRC Press, London, New York, Washington D.C..

Kuhlmann, H., Claassen, N., Wehrmann, J., 1985. A method for determining the K-uptake from subsoil by plants. Plant and Soil 83, 449-452.

Larue, J-P., Etienne, R., 2000. Les Sables de Lozère dans le Bassin parisien : nouvelles interpétations. Géologie de la France 2, 81-94.

Laskowski, R., Berg, B., Johansson, M-B., McClaugherty, C., 1995. Release pattern for potassium from decomposing forest needle and leaf litter. Long-term decomposition in a Scots pine forest. IX. Canadian Journal of Botany 73, 2019-2027.

Likens, G. E., Cowan Jr, J. H., 1992. The ecosystem approach: its use and abuse. Ecology Institute.

Marrero, S.M., Hein, A.S., Naylor, M., Attal, M., Shanks, R., Winter, K., Woodward, J., Dunning, S., Westoby, M., Sugden, D., 2018. Controls on subaerial erosion rates in Antarctica. Earth and Planetary Science Letters 501, 56-66.

Marshall., D.C.W., Bayliss, A.C., 1994. Flood estimation for small catchments. Institute of Hydrology.

Martin, J-M., Meybeck, M., 1979. Elemental mass-balance of material carried by major world rivers. Marine Chemistry 7, 173-206.

Milnes, A.R., Fitzpatrick, R.W., 1989. Titanium and zirconium minerals. Minerals in soil environments, 1131-1205.

Négrel, Ph., 1997. Multi-element chemistry of Loire estuary sediments: anthropogenic vs. natural sources. Estuarine, Coastal and Shelf Science 44 No. 4, 395-410.

Négrel, Ph., 1999. Geochemical study of a granitic area–the Margeride Mountains, France: chemical element behavior and 87Sr/86Sr constraints. Aquatic Geochemistry 5 No. 2, 125-165.

Négrel, Ph., Deschamps, P., 1996. Natural and anthropogenic budgets of a small watershed in the Massif Central (France): chemical and strontium isotopic characterization of water and sediments. Aquatic Geochemistry 2 No. 1, 1-27.

Négrel, Ph., Grosbois, C., 1999. Changes in chemical and 87Sr/86Sr signature distribution patterns of suspended matter and bed sediments in the upper Loire river basin (France). Chemical Geology 156 No. 1-4, 231-249.

Négrel, Ph., Pauwels, H., Chabaux, F., 2018a. Characterizing multiple water-rock interactions in the critical zone through Sr-isotope tracing of surface and groundwater. Applied Geochemistry 93, 102-112.

Négrel, Ph., Ladenberger, A., Reimann, C., Birke, M., Sadeghi, M., the GEMAS Project Team, 2018b. Distribution of Rb, Ga and Cs in agricultural land soils at European continental scale (GEMAS): Implications for weathering conditions and provenance. Chemical Geology 479, 188-203.

Nelson, D. J., 1973. Measurement and sampling of outputs from watersheds. In Analysis of temperate forest ecosystems, 257-267. Springer, Berlin, Heidelberg.

Nesbitt, H.W., Markovics, G., Prict, R.C., 1980. Chemical processes affecting alkalis and alkaline earths during continental weathering. Geochimica et Cosmochimica Acta 44 No. 11, 1659-1666.

Oelkers, E.H., Gislason, S.R., Eiriksdottir, E.S., Jones, M., Pearce, C.R., Jeandel C., 2011. The role of riverine particulate material on the global cycles of the elements. Applied Geochemistry 26, S365-S369.

Oludare, F.V., 2017. Effects of Weathering and Erosion on the Geochemistry Of Rocks And Soils. International Journal of Scientific Research in Science and Technology 3 No. 6, 74-80.

Palis, R.G., Okwach, G., Rose, C.W., Saffigna, P.G., 1990. Soil erosion processes and nutrient loss. 1. The interpretation of enrichment ratio and nitrogen loss in runoff sediment. Soil Research 28 No. 4, 623-639.

Parker, R.L., 1967. Composition of the earth's crust. In data of geochemistry. United States Government Printing Office.

Pickering, W.F., 1986. Metal ion speciation—soils and sediments (a review). Ore Geology Reviews 1 No. 1, 83-146.

Pierret, M.C., Cotel, S., Ackerer, P., Beaulieu, E., Benarioumlil, S., Boucher, M., Boutin, R., Chabaux, F., Delay, F., Fourtet, C., Friedmann, P., Fritz, B., Gangloff, S., Girard, J-F., Legtchenko, A., Viville, D., Weill, S., Probst, A., 2018. The Strengbach catchment: A multidisciplinary environmental sentry for 30 years. Vadose Zone Journal 17 No. 1.

Pollet, E., 2009. Vademecum des sols hydromorphes. Office national de l'eau et des milieu aquatiques,.

Poszwa, A., Dambrine, E., Pollier, B., Atteia, O., 2000. A comparison between Ca and Sr cycling in forest ecosystems. Plant and Soil 225 No. 1-2, 299-310.

Reimann, C., de Caritat, P., 2000. Intrinsic flaws of element enrichment factors (EFs) in environmental geochemistry. Environmental Science & Technology 34 No. 24, 5084-5091.

Reimann, C., Filzmoser, P., Garrett, R. G., 2002. Factor analysis applied to regional geochemical data: problems and possibilities. Applied geochemistry 17 No. 3, 185-206.

Reimann, C., de Caritat, P., 2005. Distinguishing between natural and anthropogenic sources for elements in the environment: regional geochemical surveys versus enrichment factors. Science of the Total Environment 337 No. 1-3, 91-107.

Reimann, C., Birke, M., Demetriades, A., Filzmoser, P., O'Connor, P. (Eds.), 2014a. Chemistry of Europe's Agricultural Soils - Part A: Methodology and Interpretation of the GEMAS dataset. Geologisches Jahrbuch (Reihe B). Schweizerbarth, Stuttgart 528 pp.

Reimann, C., Birke, M., Demetriades, A., Filzmoser, P., O'Connor, P. (Eds.), 2014b. Chemistry of Europe's Agricultural Soils - Part B: general background information and further analysis of the GEMAS dataset. Geologisches Jahrbuch (Reihe B). Schweizerbarth, Stuttgart 352 pp.

Richter, D.D., Bacon, A.R., Brecheisen, Z., Mobley, M.L., 2015. Soil in the Anthropocene. IOP Conference Series: Earth and Environmental Science 25 No. 1.

Richter, D.D., Billings, S.A., 2015. 'One physical system': Tansley's ecosystem as Earth's critical zone. New Phytologist 206 No. 3, 900-912.

874 Righi, D., Meunier, A., 1995. Origin of clays by rock weathering and soil formation. In Origin and
875 mineralogy of clays. Springer, Berlin.

876 Rowntree, K.M., Ntsaba, M.M, Van B. Weaver, A., 1991. Changing patterns of erosion in a peri-urban
877 catchment, Maseru, Lesotho. International Association of Hydrological Sciences Publications No. 203.

878 Sawhney, B.L., 1972. Selective sorption and fixation of cations by clay minerals: a review. Clays and clay
879 minerals 20 No. 2, 93-100.

880 Silva, S.H.G., Hartemink, A.E., dos Santos Teixeira, A.F., Inda, A.V., Guilherme, L.R.G., Curi, N.,
881 2018. Soil weathering analysis using a portable X-ray fluorescence (PXRF) spectrometer in an
882 Inceptisol from the Brazilian Cerrado. Applied Clay Science 162, 27-37.

883 Soucémarianadin L., Verbèque, B., 2007. Notice explicative de la carte des sols de Orléans (1/50 000).
884 Chambre d'argriculture du Loiret, Orléans.

885 Sucharovà, J., Suchara, I., Hola, M., Marikova, S., Reimann, C., Boyd, R., Filzmoser, P., Englmaier,
886 P., 2012. Top-/bottom-soil ratios and enrichment factors: what do they really show?. Applied
887 Geochemistry 27 No. 1, 138-145.

888 Viers, J., Dupré, B., Gaillardet, J., 2009. Chemical composition of suspended sediments in World
889 Rivers: New insights from a new database. Science of the total Environment 407 No. 2, 853-868.

890 Wilson, M. C., & Jackson, L. E., 2016. Urban geology: An emerging discipline in an increasingly
891 urbanized world. Earth magazine March 2016, 34-41.

892 Yang, J.L., Zhang, G.L., 2019. Si cycling and isotope fractionation: Implications on weathering and
893 soil formation processes in a typical subtropical area. Geoderma 337, 479-490.

894 Zhang, C., Selinus, O., 1998. Statistics and GIS in environmental geochemistry—some problems and
895 solutions. Journal of Geochemical Exploration 64 No. 1-3, 339-354.
896

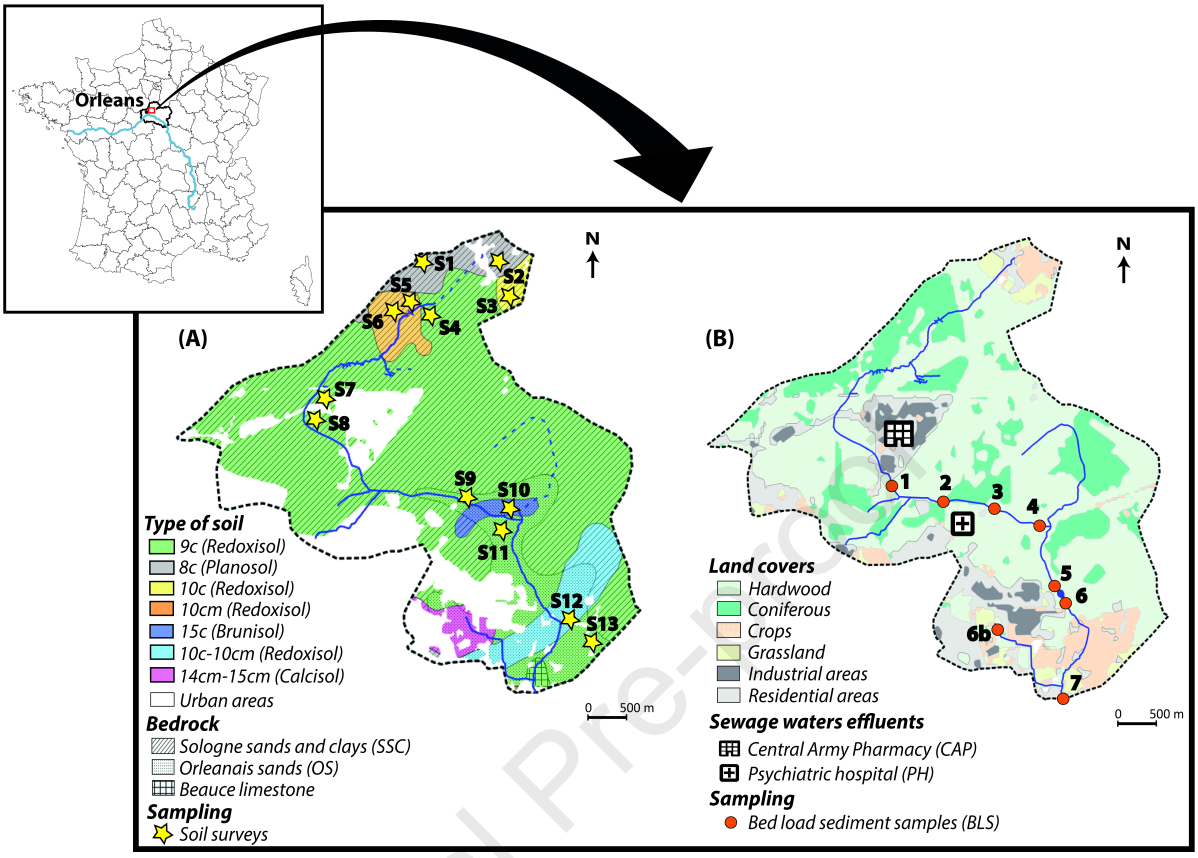

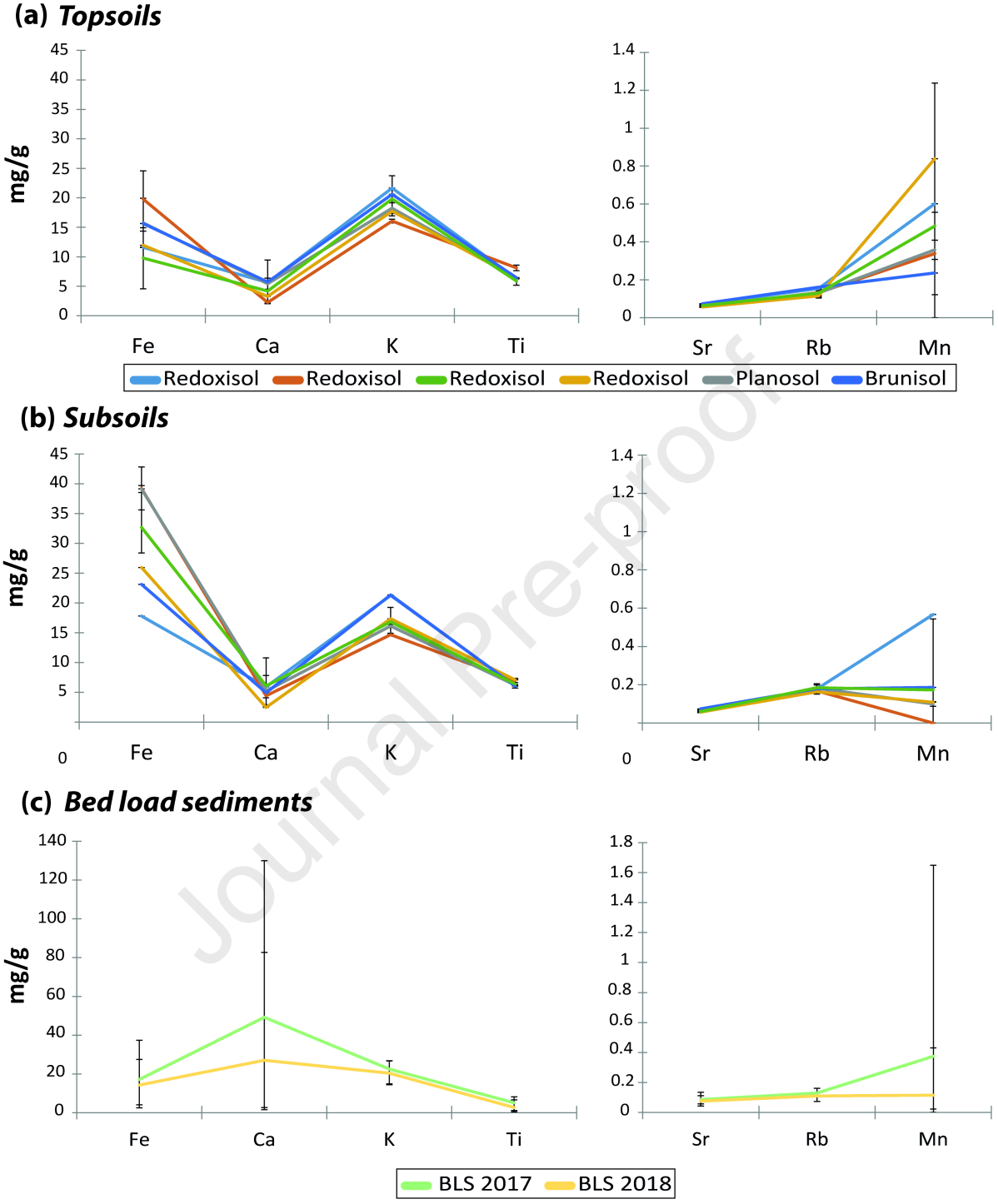

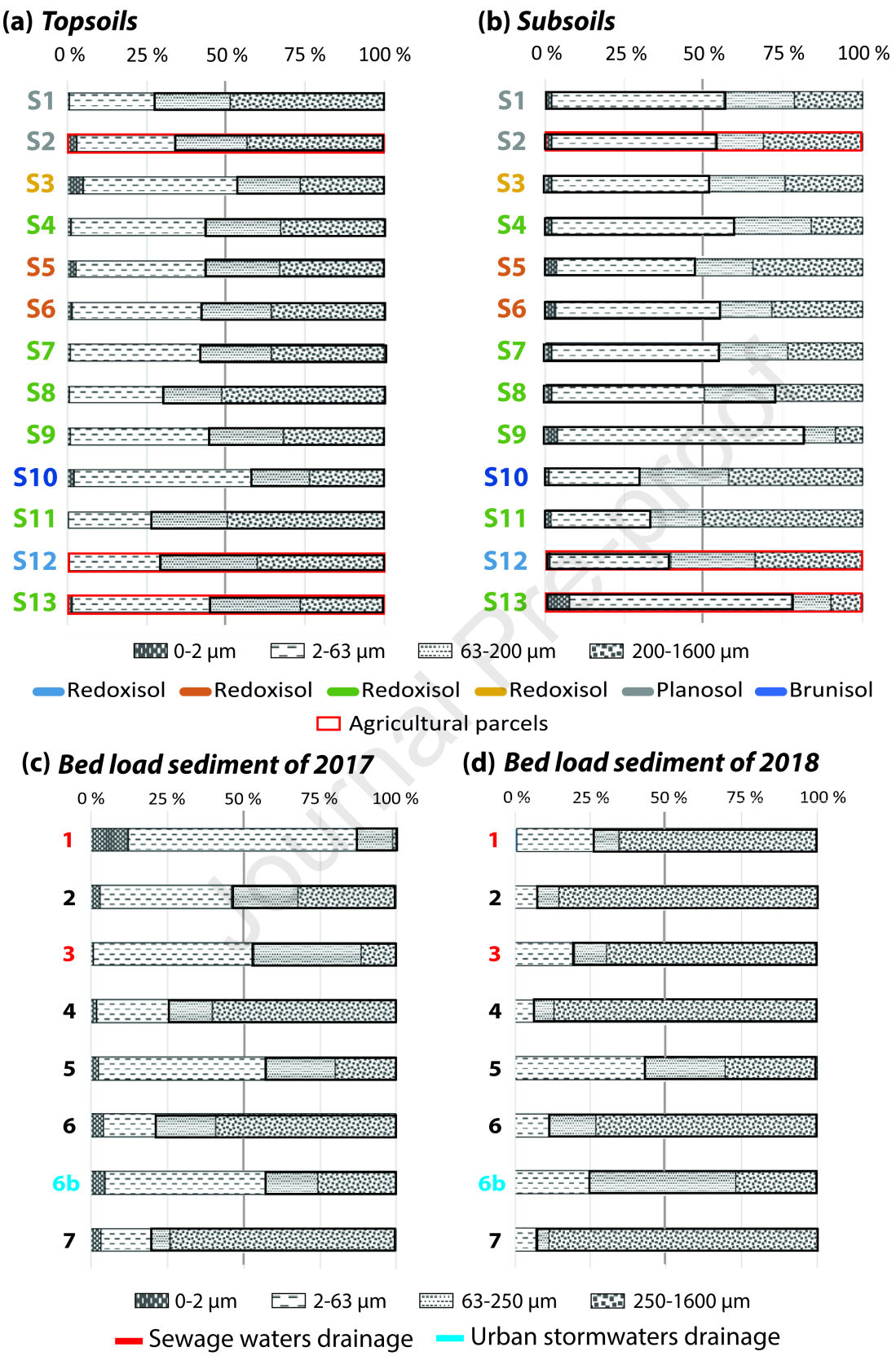
(a) Topsoils
0 %
25 %
50 %
75 %
100 %
S1
S2
S3
S4
S5
S6
S7
S8
S9
S10
S11
S12
S13
(b) Subsoils
0 %
25 %
50 %
75 %
100 %
S1
S2
S3
S4
S5
S6
S7
S8
S9
S10
S11
S12
S13
0-2 µm
2-63 µm
63-200 µm
200-1600 µm
Redoxisol
Redoxisol
Redoxisol
Redoxisol
Planosol
Brunisol
Agricultural parcels
(c) Bed load sediment of 2017
0 %
25 %
50 %
75 %
100 %
1
2
3
4
5
6
6b
7
(d) Bed load sediment of 2018
0 %
25 %
50 %
75 %
100 %
1
2
3
4
5
6
6b
7
0-2 µm
2-63 µm
63-250 µm
250-1600 µm
Sewage waters drainage
Urban stormwaters drainage

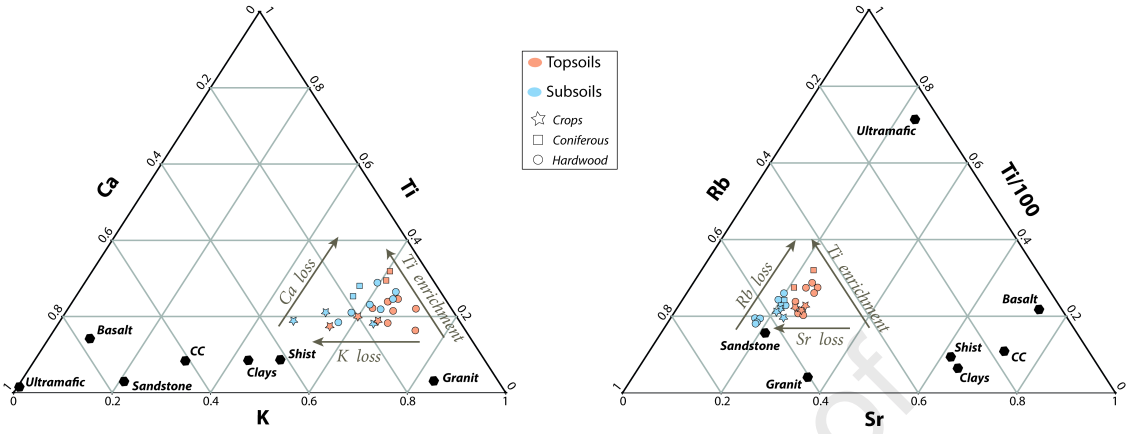

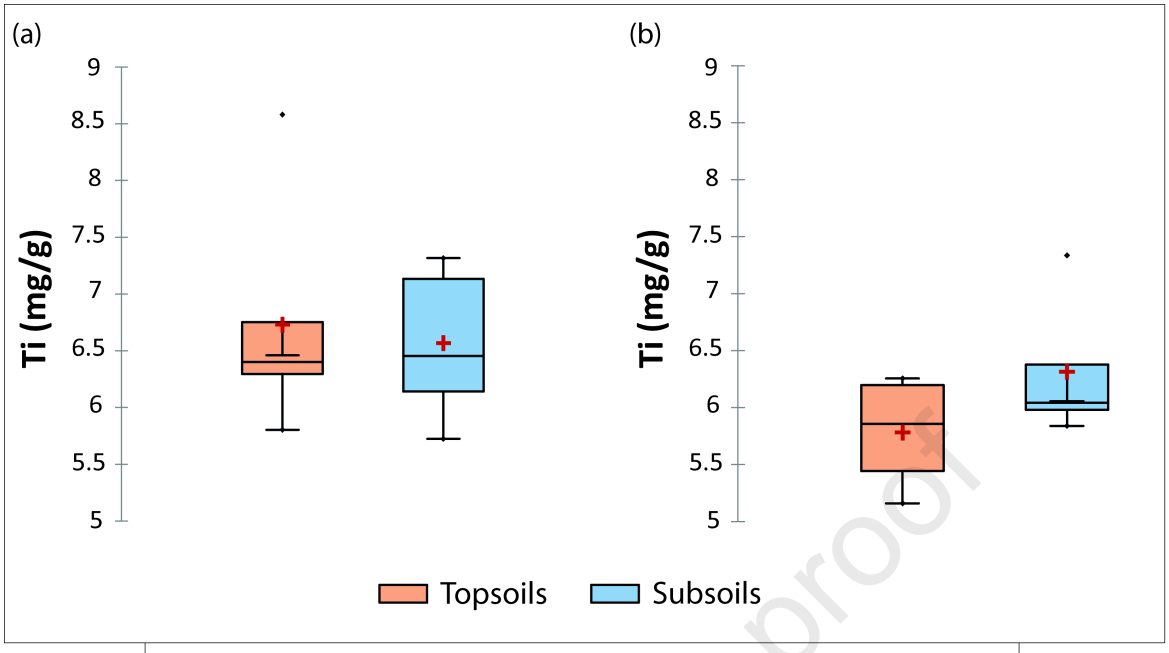

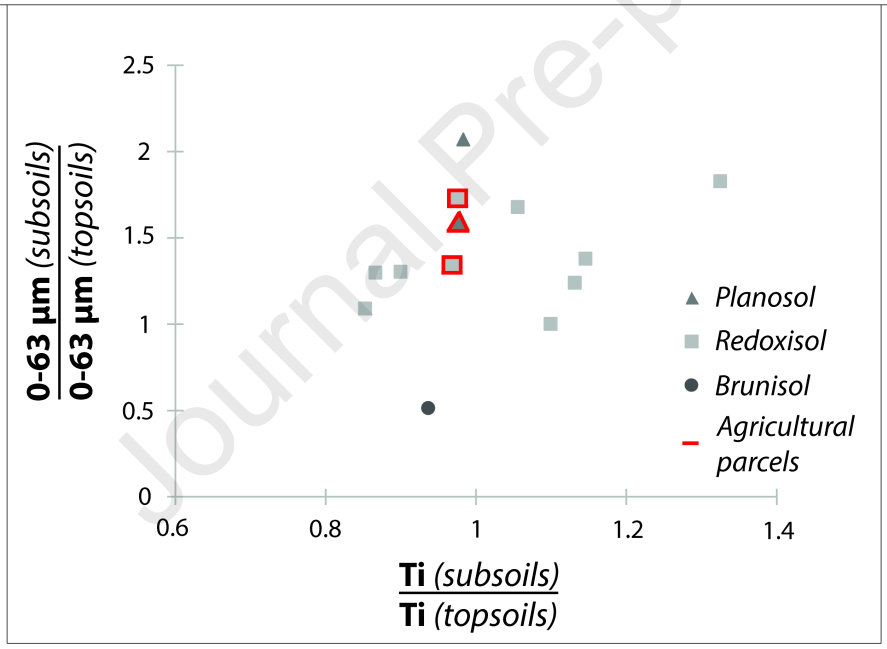

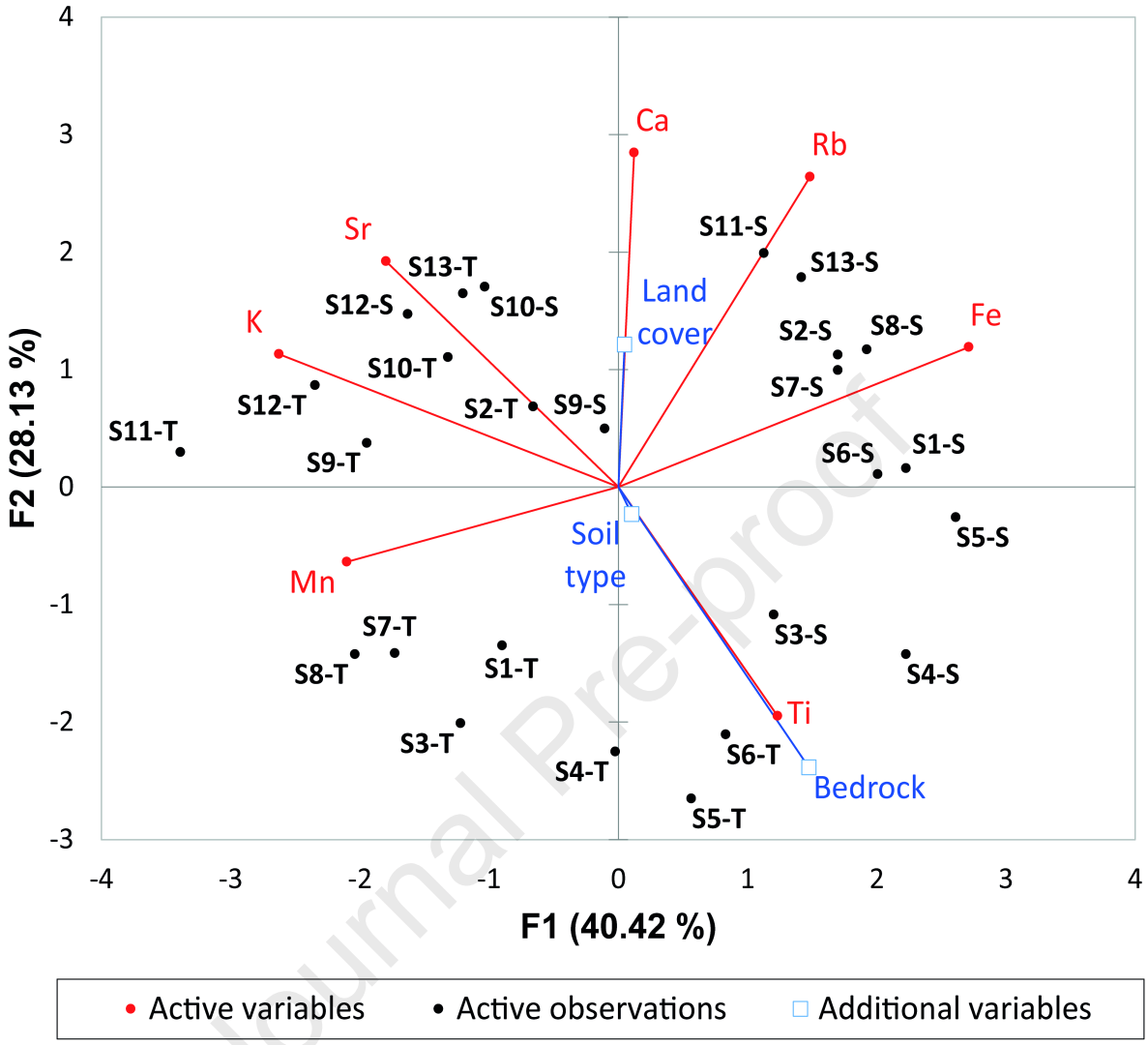

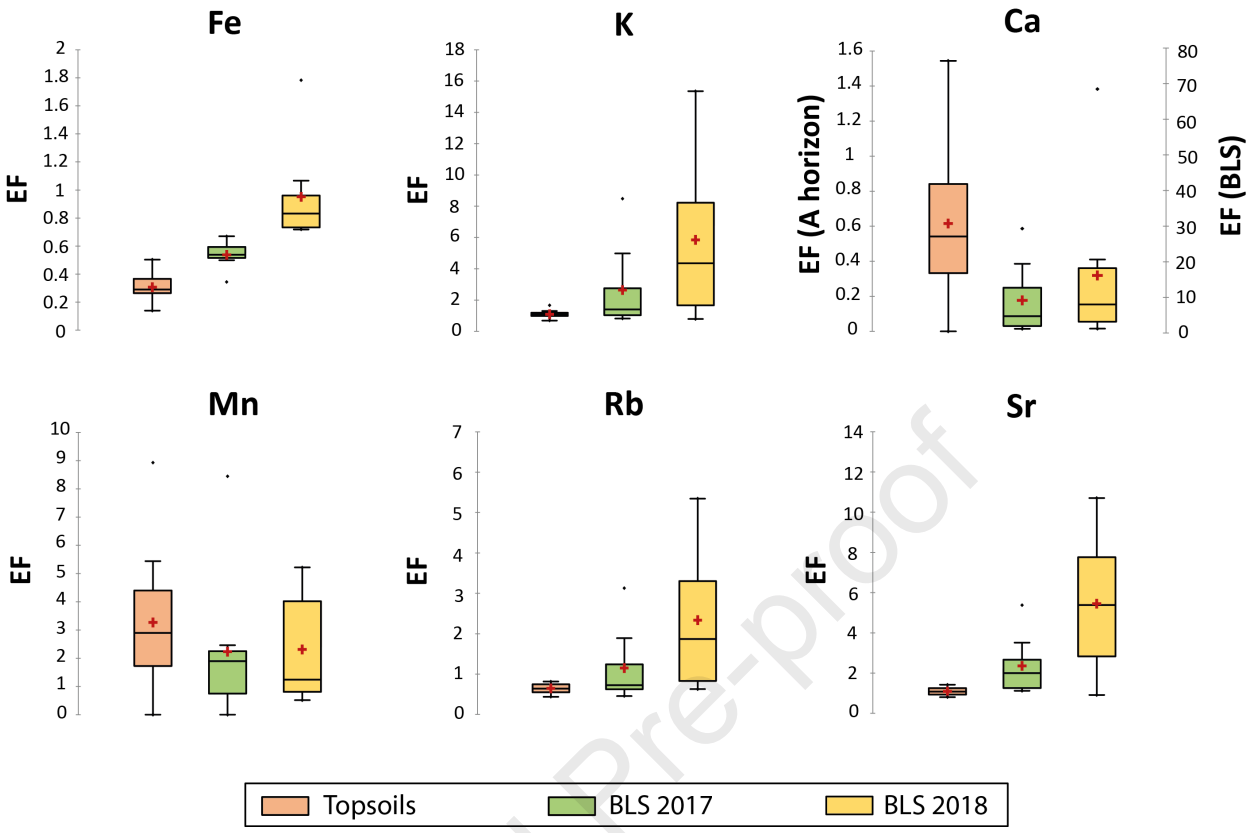

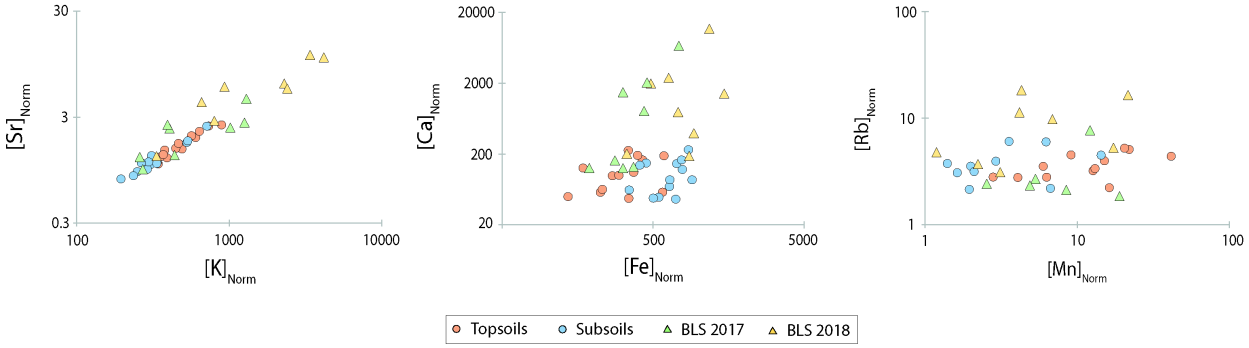

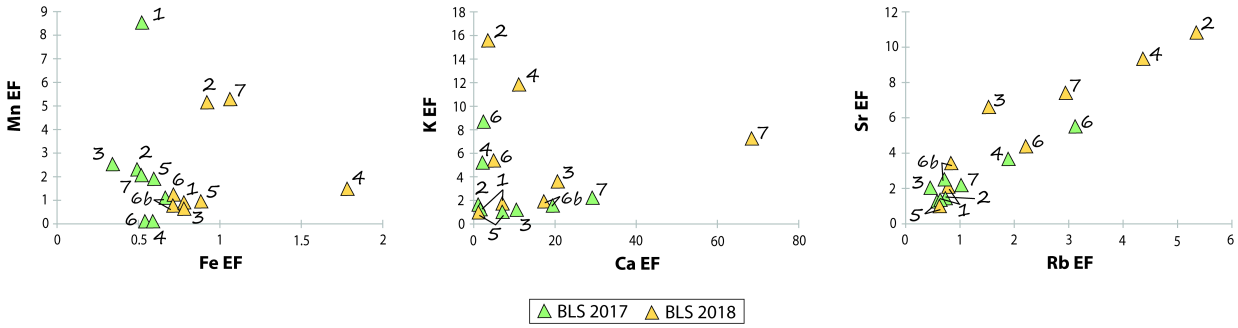

Highlights

- Geochemical effects of silicate weathering and erosion continuum processes
- Hydromorphic soils slow weathering allows detailed forcing factors visualizing
- Particles sources, erosion selectivity, disaggregation and rates drive sediment geochemistry
- Stream transportation/deposition dynamic controls sediment geochemistry temporal evolution
- Sediment geochemistry is modified by stormwaters contributions from urban areas

Declaration of interests

☒ The authors declare that they have no known competing financial interests or personal relationships that could have appeared to influence the work reported in this paper.

☐The authors declare the following financial interests/personal relationships which may be considered as potential competing interests: